AD-A207 312

Navy Tethered Balloon Measurements Made During the "Fire" Marine Stratocu IFO July 1987

JEFFREY E. JAMES, H. GERBER AND S. G. GATHMAN

Atmospheric Physics Branch
Space Science Division

MIKE SMITH AND IAN CONSTERDINE

Institute of Science and Technology
University of Manchester
Manchester, England

DTIC
ELECTE
APR 26 1989
D

April 3, 1989

REPORT DOCUMENTATION PAGE

Form Approved
OMB No 0704-0188

1a REPORT SECURITY CLASSIFICATION	1b RESTRICTIVE MARKINGS
UNCLASSIFIED	

2a SECURITY CLASSIFICATION AUTHORITY	3 DISTRIBUTION/AVAILABILITY OF REPORT
2b DECLASSIFICATION/DOWNGRADING SCHEDULE	Approved for public release; distribution unlimited.

4 PERFORMING ORGANIZATION REPORT NUMBER(S)	5 MONITORING ORGANIZATION REPORT NUMBER(S)
NRL Memorandum Report 6445	

6a NAME OF PERFORMING ORGANIZATION	6b OFFICE SYMBOL (If applicable)	7a NAME OF MONITORING ORGANIZATION
Naval Research Laboratory	Code 4110	

6c ADDRESS (City, State, and ZIP Code)	7b ADDRESS (City, State, and ZIP Code)
Washington, DC 20375-5000	

8a NAME OF FUNDING/SPONSORING ORGANIZATION	8b OFFICE SYMBOL (If applicable)	9 PROCUREMENT INSTRUMENT IDENTIFICATION NUMBER
Naval Ocean Systems Command	Code 54	

8c ADDRESS (City, State, and ZIP Code)	10 SOURCE OF FUNDING NUMBERS			
	PROGRAM ELEMENT NO	PROJECT NO	TASK NO	WORK UNIT ACCESSION NO
San Diego, CA 92152-5000	62435N	RA35G80	N01A	DN880-082

11 TITLE (Include Security Classification)

Navy Tethered Balloon Measurements Made During the "Fire" Marine Stratocu IFO - July 1987

12 PERSONAL AUTHOR(S)
James, J.E., Gerber, H., Gathman, S.G., Smith,* M. and Consterdine,* I.

13a TYPE OF REPORT	13b TIME COVERED FROM ___ TO ___	14 DATE OF REPORT (Year, Month, Day) 1989 April 3	15 PAGE COUNT 127

16 SUPPLEMENTARY NOTATION
*Institute of Science and Technology, University of Manchester, Manchester, England

17	COSATI CODES		18 SUBJECT TERMS (Continue on reverse if necessary and identify by block number)
FIELD	GROUP	SUB-GROUP	
			(See page ii)

19 ABSTRACT (Continue on reverse if necessary and identify by block number)

For a ten-day period beginning 15 July 1987, tethered balloon measurements were made of turbulence, aerosol, cloud particles, and meterorology at San Nicolas Island, CA during the FIRE marine strato-cumulus Intensive Field Operation (IFO). The primary interest of the Naval Research Laboratory during this experiment was to obtain a data set which could be used for testing the predictions of the Navy Oceanic Vertical Aerosol Model (NOVAM) which describes the atmosphere's optical/IR properties in terms of easily obtained meterological data. Two new instruments, flown aboard the balloon, were a saturation hygrometer, which measures 95% < RH < 150% with an accuracy of 0.05% near 100% RH, and a forward scatter meter which gives in situ measurements of liquid water content at more than 10 Hz. As a result of this experiment a unique and greatly improved look at the microphysics of the clear and cloud topped boundary layer can be taken. In this report the quality of the data obtained is discussed and some preliminary results are given. Algorithms for the instrumentation flown aboard the balloon are given and profiles of some of the measurements made are shown.

20 DISTRIBUTION/AVAILABILITY OF ABSTRACT	21 ABSTRACT SECURITY CLASSIFICATION
☒ UNCLASSIFIED/UNLIMITED ☐ SAME AS RPT ☐ DTIC USERS	UNCLASSIFIED

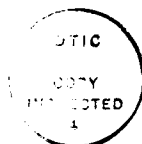| 22a NAME OF RESPONSIBLE INDIVIDUAL	22b TELEPHONE (Include Area Code)	22c OFFICE SYMBOL
J. James	(202) 767-2022	Code 4117

DD Form 1473, JUN 86 — Previous editions are obsolete — SECURITY CLASSIFICATION OF THIS PAGE

S/N 0102-LF-014-6603

18. SUBJECT TERMS

Relative humidity profiles
Temperature profiles
Liquid water profiles
Liquid water content
Wind speed profiles
Tethered balloon
Aerostat
FIRE marine stato cumulus IFO
Saturation hygrometer
Forward scatter meter
Nephelometers
Aerosol
Particle spectrometer
Strato cumulus
Boundary layer
Collocated measurements
Orthogonal transformation

Accesion For		
NTIS CRA&I	☑	
DTIC TAB	☐	
Unannounced	☐	
Justification		

By
Distribution /

Availability Codes		
Dist	Avail and / or Special	
A-1		

CONTENTS

NAVY TETHERED BALLOON MEASUREMENTS MADE DURING THE "FIRE" MARINE STRATOCU IFO — JULY 1987

INTRODUCTION

A series of tethered balloon measurements were made by the Naval Research Laboratory (NRL) from 15 July to 25 July during the FIRE marine strato-cumulus Intensive Field Operation (IFO) held at San Nicolas Island (SNI), California. Several groups were involved in the field experiment including scientists from NRL, National Aeronautics and Space Administration (NASA), Penn State (PSU), The University of Manchester, England (UMIST), Naval Ocean Systems Command (NOSC), National Oceanic and Atmospheric Administration (NOAA), Colorado State University (CSU), the Naval Post Graduate School (NPS), and the University of Denver.

Collocated measurements of turbulence, aerosol, cloud particles, and meteorology were made below, within, and above the marine boundary layer with the instruments mounted on a platform that hung 35-m below the balloon. The instrument suite included two new instruments that were expected to make significant contributions to this effort. These instruments were the saturation hygrometer (Gerber, 1980) capable of measuring 95%< RH <105% (with an accuracy of 0.05% near 100%) and used for the first time in clouds, and the forward scatter meter (Gerber, 1987), which gives in situ LWC measurements at more than 10 Hz.

A specific goal of the NRL balloon measurements was to obtain a data set that could be used to test the predictions of the Navy Oceanic Vertical Aerosol Model (NOVAM). NOVAM is a computer program that predicts the vertical structure of the atmosphere's optical/IR properties based on easily obtained meteorological data. NOVAM is the result of cooperation between NRL, NOSC, and NPS and is a product of the Navy's EOMET program. The present version of NOVAM is written in Turbo PASCAL and will run on IBM and IBM-compatible computers. A report describing the present version of NOVAM is due to be released in the near future, Gathman(1989).

The NOVAM model will be tested by using the meteorological measurements obtained from the experiment as input data for the model and then comparing the IR extinction profiles as calculated from the measured aerosol size distributions with the IR extinction profiles predicted by NOVAM. Similarly, the visible extinction measurement profiles will be compared with the visible profiles predicted by NOVAM.

Another result of this experiment is that a data set has been obtained that provides a unique and greatly improved look at the microphysics of the clear and cloud topped boundary layer.

This report discusses the measurements made by the NRL package, data reduction and data quality. Profiles are given of wind speed, liquid water content, dry bulb temperature, dry bulb-wet bulb temperature, and time.

EXPERIMENT AT SNI

SNI lies 102-km south-southwest of Pt. Mugu, California. It has an area of approximately 50 square km with a length of 14.5-km and a width of 5-km. Figure 1 shows the location of SNI with respect to the mainland.

The NRL balloon launch site was located at the northwest tip of the island approximately 50 ft above sea level. Figure 2 shows the launch site as well as some other important locations.

The FIRE experiment was conducted from 1 July until 19 July. Technical problems prevented NRL balloon measurements from being made until late in the IFO period. The first NRL balloon flight took place on 15 July. Because of the late start, measurements were made for an additional week after other FIRE investigators had left. Seventeen flights were made over a 10-day period from 15 July through 25 July. The typical flight lasted approximately 3 h with an initial ascent of 0.5 m/s to the free atmosphere above the boundary layer. Several stops were made during the descent of the balloon, lasting about 25 min each, to obtain turbulence statistics. Table 1 summarizes the duration and local meteorology for each of the 17 flights.

The meteorology during the additional week following 19 July was characterized by several episodes of fractional strato-cumulus cloud cover, which were mostly missing earlier in the IFO period. Two such episodes occurred on the morning flight of 23 July when the cloud cover was rapidly decreasing, and on the morning flight of 24 July when the opposite trend occurred. A study of relationship between turbulence and microphysics for these two fractional-cloudy cases would address a goal of FIRE: to understand the factors that cause the formation and evolution of fractional strato-cumulus cloud cover.

Among the instrumentation, which was operated on the island, were a wind profiler and photometers operated by Fairall (PSU) and a microwave radiometer operated by Snider (NOAA). Measurements were collected aboard the Point Sur upwind of SNI from 4 July through 17 July. Some of the instrumentation aboard the Point Sur included a forward scatter meter, which unfortunately had problems and did not yield any usable data, an HSS visibility meter, a radon concentration measuring device to determine the continental influence on the surrounding marine atmosphere, a CSASP particle spectrometer, SODAR, and other meteorological instrumentation.

Several flights were made upwind of SNI by the NOSC Navahoe Piper Cub in the week following 19 July. Among the measurements taken aboard the aircraft were sea-surface temperature, particle-size spectra, and meteorological variables.

INSTRUMENT DESCRIPTION

The NRL aerostat consists of a 19,000 ft^3 balloon, with a lifting capability of 500 lb, and a flat bed trailer on which is mounted a pivotable mooring system as shown in Fig. 3. The tail of the mooring system acts as a wind vane, which keeps the balloon and mooring system facing into the wind. A variable

2
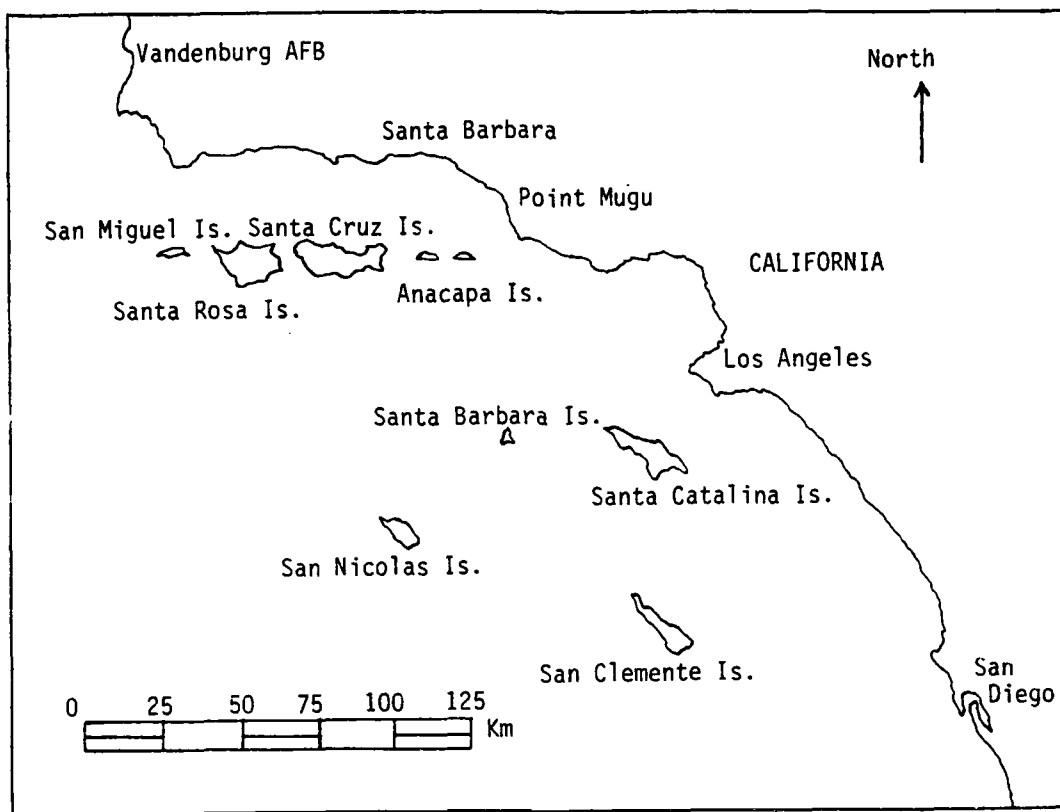
Fig. 1 Location of San Nicolas Island with respect to the mainland.
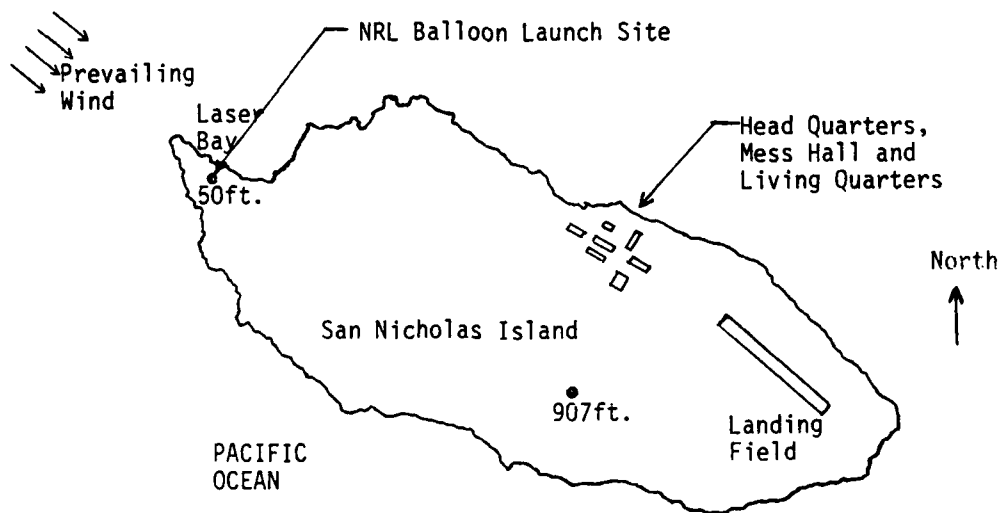
Fig. 2 Important sites on San Nicolas Island.

3
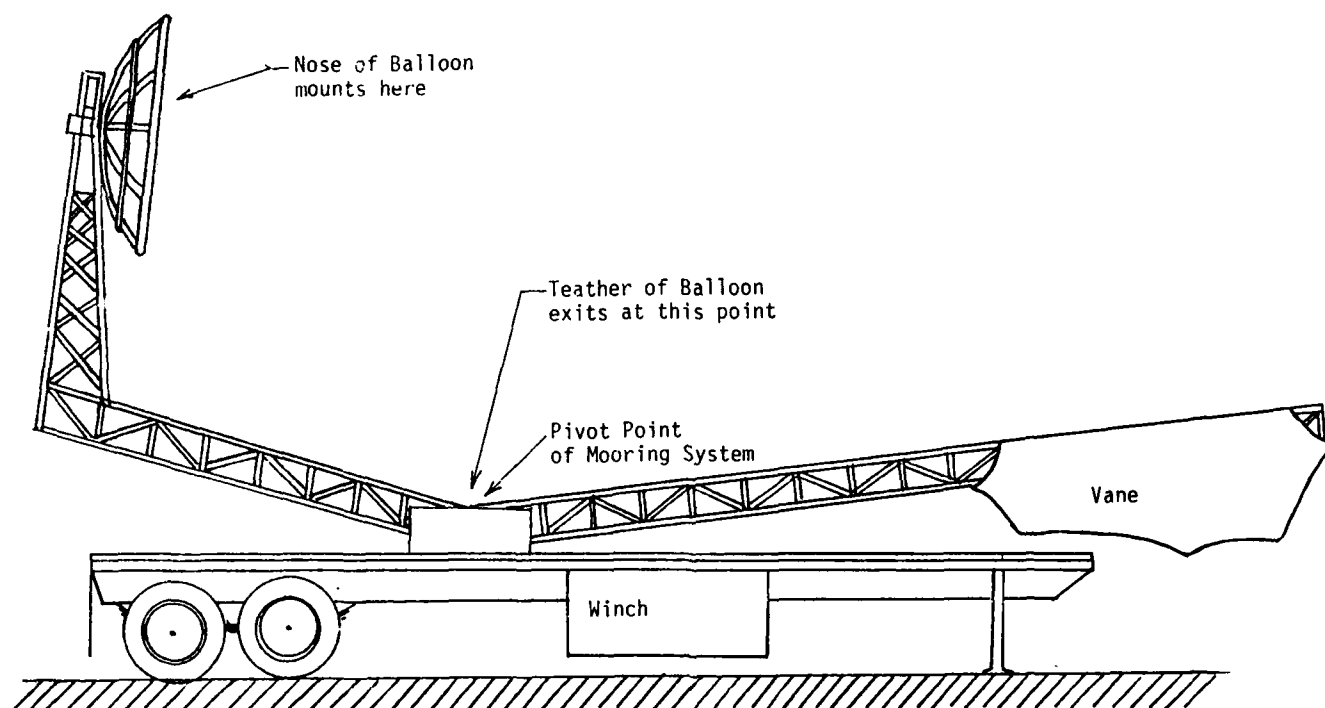
Fig. 3 Mooring system of the NRL aerostat.

Flt. No.	Flt. Name	Date	Duration of Flight	Cloud Cover		Wind Dir.	Sfc. Wind (m/s)	Inversion Ht. (m)
1	1515	15/7/87	1511-1707	10/10		NW	7	640
2	1609	16/7/87	0900-1140	10/10		W	2	760
3	1617	16/7/87	1737-1930	10/10		W	2	-
4	1710	17/7/87	1100-1415	10/10-5/10	(d)	NW	9	1070
5	1807	18/7/87	0735-1115	1/10		WNW	2	670
6	1814	18/7/87	1407-1552	0/10		NW	5-7	400
7	195	19/7/87	0522-0706	<1/10		NW	5-7	335
8	1913	19/7/87	1332-1559	<<1/10		NW	2-4	460
9	2008	20/7/87	0817-1013	6/10-1/10	(d)	WNW	5-7	640
10	2017	20/7/87	1803-1945	0/10		WNW	5	-
11	2112	21/7/87	1305-1535	0/10		WNW	<2	-
12	2217	22/7/87	1744-1946	0/10		NW	7	380
13	239	23/7/87	0952-1225	8/10-1/10	(d)	NW	9	640
14	2315	23/7/87	1518-1648	0/10		NW	9-13	-
15	247	24/7/87	0756-1101	6/10-10/10	(i)	NW	7-9 (d)	550
16	2417	24/7/87	1723-1945	1/10-4/10		NW	9	360
17	257	25/7/87	0815-1026	1/10-5/10		NW	7	400

(d-decreasing, i-increasing)

Table 1. Summary of flights and local meteorology.

4

speed winch is mounted underneath the trailer. The balloon is attached to the mooring system by a tether that is controlled by the winch.

The NRL instrument package shown in Fig. 4 hangs 35-m below the balloon on its own support line. Data and power cables run the length of the support line Power is supplied by a gas powered AC generator that is mounted to the base of the balloon. A telemetry unit mounted on the balloon, which sends information relating to the operation of the balloon to an LTA balloon monitoring system, was used to send several data channels from the instrument package to an NRL ground station so data such as altitude, liquid water content and dry bulb-wet bulb temperature could be monitored in real time. The NRL ground station used an IBM-compatible personal computer to display and log these data in real time The instrument package data logger was also an IBM PC clone. A data logging program was written that would automatically begin data logging when power was applied to the instrument package. Data were stored in an extended RAM in a compressed binary format. At the end of each flight the ground-station PC was connected to the instrument-package PC through an RS232C serial communications interface. The data were then transferred from the instrument package data logger at high speed to a 20 MB removable hard disk.

A support line package, which was mounted approximately 2-m below the confluence point of the balloon included two inclinometers mounted at right angles to each other and a flux gate magnetometer. These used in conjunction with the altimeter and a second flux gate magnetometer mounted on the instrument package yield a positioning system with which an orthogonal transformation of the velocity vector measured by the bivane anemometer can be made to correct for the motion of the package.

The motion of the instrument package during flight was well behaved. The intermittent motion of the package was noted to be perpendicular to the wind direction with a period of oscillation of 11.8 s.

Following is a description of each instrument that was flown aboard the instrument package and their respective reducing algorithms. Table 2 lists the instrumentation and the rates at which they were sampled.

Psychrometer Dry Bulb, *Td* (°C)

This psychrometer is described in Gerber (1986). The accuracy of *Td* is ± 0.15 °C, except when the thermistor is wetted by cloud droplets. The 1/e time response is 3 s.

$$Td = \frac{C}{0.1V} V1 \tag{1}$$

where *V1* is the output voltage of the psychrometer dry bulb stored in the data file OUTXXYY.PDB, *XX* is a number that corresponds to the day of the flight and *YY* is a number that corresponds to the hour the flight started.

Some radio frequency (RF) noise from the LTA telemetry system affected the quality of this data. By averaging the raw data over 1 s the effects of the noise are greatly reduced.

Altimeter and Telemetry System

Power Generator

Inclinometer #1
Inclinometer #2
Support Line Compass

Inclinometer#1
Inclinometer#2
Compass
Altimeter

FSM
Dry-WetTemperature

CSASP
Forward Scatter Meter(LWC)
Psychrometer
Saturation Hygrometer
Nephelometer
Ozone Meter
Pallet Compass
Bivane Anemometer
Video Camera
Data Logger

35m

Vane

Pallet
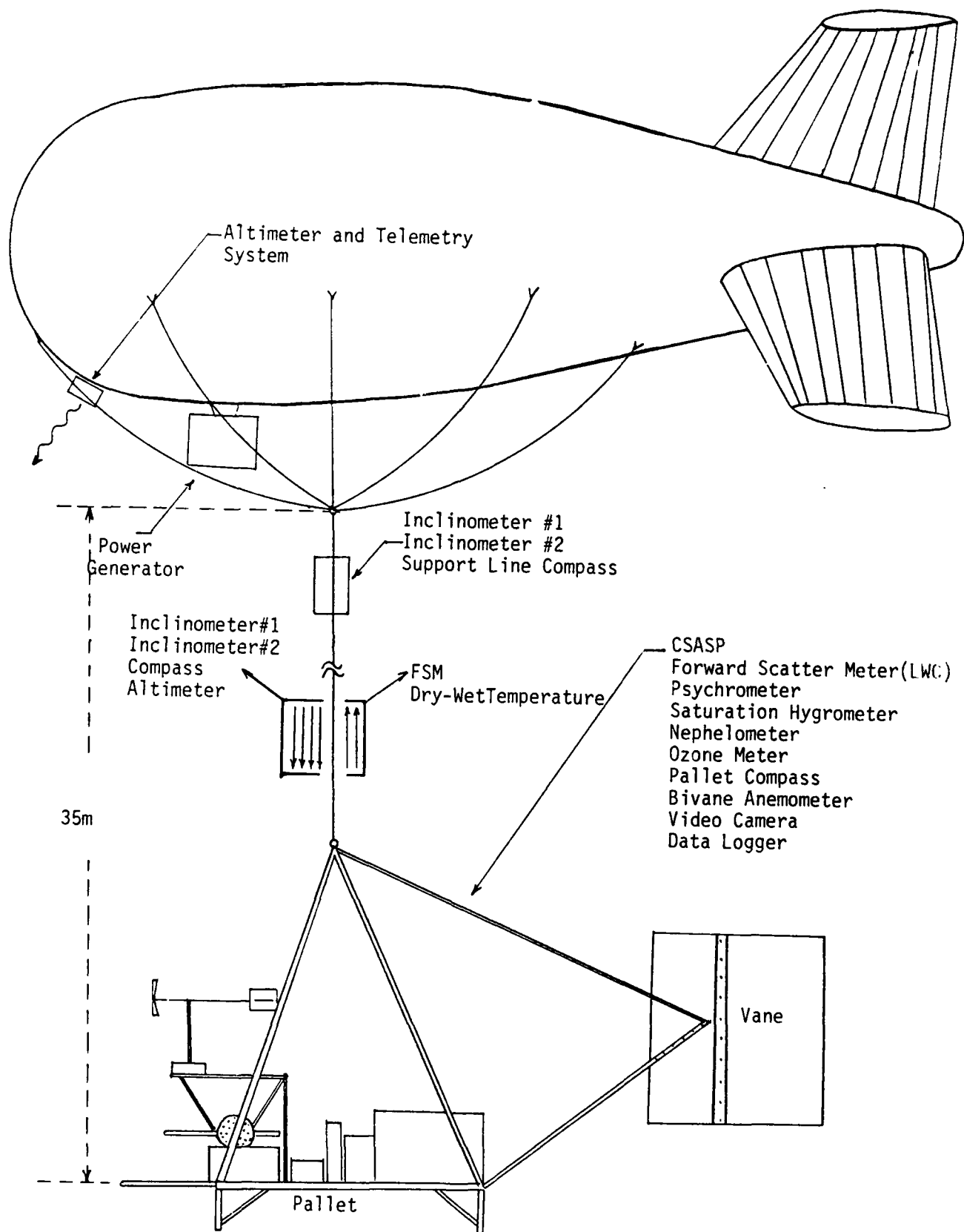
Fig. 4 NRL Instrument package and balloon.

6

No.	Instrument	Location Recorded	Rate Sampled
1	Psychrometer, Dry Bulb Temp.	IP	5Hz
2	Psychrometer, Dry Bulb-Wet Bulb Temp.	IP,GS	5Hz,.3Hz
3	Saturation Hygrometer, 95%<RH<100%	IP	5Hz
4	Saturation Hygrometer, RH>100%	IP	5Hz
5	Forward Scatter Meter, Liquid Water Cont.	IP,GS	5Hz,.3Hz
6	Bivane Anemometer, Wind Speed	IP	5Hz
7	Bivane Anemometer, Azimuth	IP	5Hz
8	Bivane Anemometer, Elevation	IP	5Hz
9	Nephelometer, Visual Scattering Coefficient	IP	1Hz
10	Ozone Meter	IP	1Hz
11	Altimeter, Balloon Altitude	IP,GS	1Hz,.3Hz
12	CSASP Particle Spectrometer	IP	1Hz
13	Clock, Time in Seconds	IP	5Hz
14	Support Line Compass	IP	1Hz
15	Pallet Compass	IP	1Hz
16	Support Line Inclinometer #1	IP	1Hz
17	Support Line Inclinometer #2	IP	1Hz
18	Video Camera	IP	N

(IP-Instrument Package Data Logger, GS-Ground Station
Data Logger, N-Normal Speed)

Table 2. List of instrument tion flown on NRL aerostat and the
rates at which they were sampled.
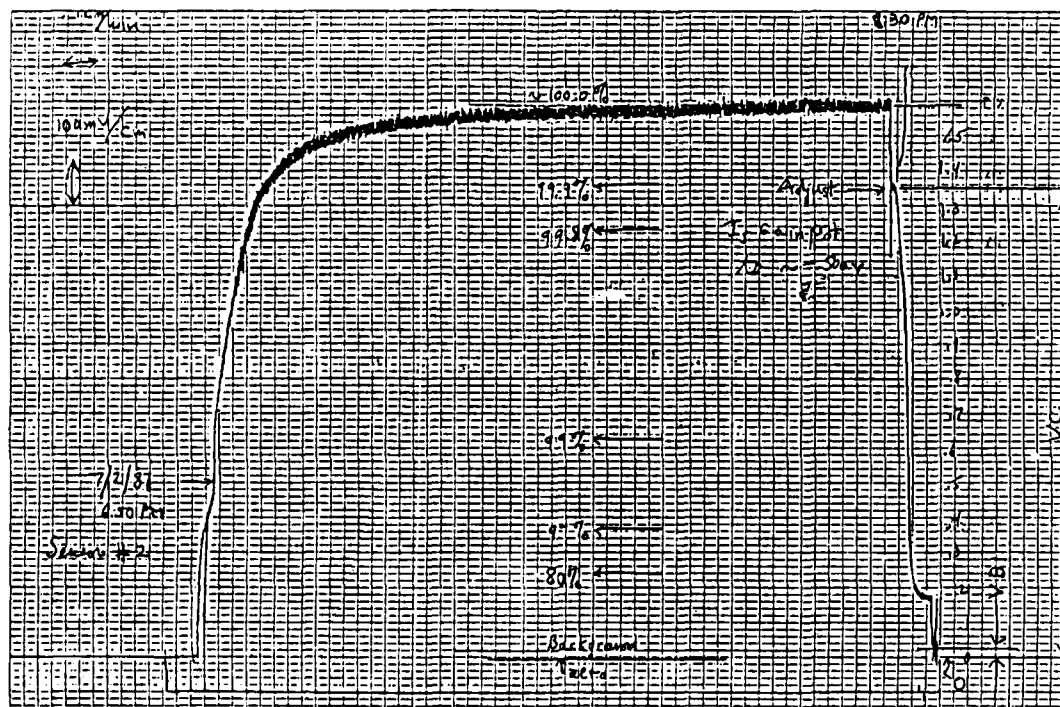
Fig. 5 Field calibration in the wet box of the saturation hygrometer.

Psychrometer Dry Bulb - Wet Bulb, $\Delta T = Td\text{-}Tw$ (°C)

This is the same instrument as described above. The thermistors were matched to within 0.002 °C. The thermistors are self aspirated in a dual radiation shield. The accuracy of RH determined from ΔT is better than 0.5%, except when the dry bulb thermistor becomes wet.

$$\Delta T = \frac{C}{0.5V} \; V2 \qquad\qquad (2)$$

where $V2$ is the output voltage stored in the data file OUTXXYY.PDT.

Saturation Hygrometer, $RH1$ (RH ≤ 100%)

This instrument is described in Gerber (1980).

$$RH1 = 0.97881 \; [\ln(R) + 102.165], \qquad\qquad (3)$$

for $0.6 < R \leq 1.0$ or $99.5\% < RH1 \leq 100.0\%$.

$$RH1 = 1.3563 \; [\ln(R) + 73.8724], \qquad\qquad (4)$$

for $0.415 < R \leq 0.6$ or $99.0\% < RH1 \leq 99.5\%$.

$$RH1 = 3.4895 \; [\ln(R) + 29.2501], \qquad\qquad (5)$$

for $0.27 < R \leq 0.415$ or $97.5\% < RH1 \leq 99.0\%$.

$$RH1 = 27.027 \; (R + 3.3375), \qquad\qquad (6)$$

for $0.233 < R \leq 0.27$ or $96.5\% < RH1 \leq 97.5\%$.

R is given by:

$$R = \frac{V3 - VB1}{VC - VB1} \qquad\qquad (7)$$

where $V3$ is the output voltage stored in the data file OUTXXYY.SHI,

$VB1$ is the background voltage, and

VC is the calibration voltage.

$VB1$ and VC must be determined for each flight with a field calibration.

Figure 5 gives an example of such a calibration where the hygrometer was placed in the wet box to determine its response to RH = 100%. Table 3 gives values of $VB1$ and VC determined for several flights.

The accuracy of the RH measurements for RH ≤ 100% were previously established from measurements by using the hygrometer in radiation fogs. Table 4 lists these accuracies.

8

Flight	VB1 (Volts)	VC (Volts)	Comments
2112	0.02	1.35	
2217	0.02	1.28	
239	0.02	1.28	Use 0.06 for VB1 and 1.15 for VC after the initial ascent of flight.
2315	0.06	1.15	
247	0.06	1.26	Use 1.15 for VC after the initial ascent of the flight.
2417	0.02	1.34	
257	0.07	1.33	

Table 3. List of *VB1* and *VC* determined for several flights.

RH	Uncertainty in RH
100%	± 0.02%
99%	± 0.1%
98%	± 0.3%
97%	± 0.6%

Table 4. Accuracy of RH measurements for RH<100% established by using the saturation hygrometer in radiation fogs.

RH	Uncertainty in RH	Comments
100%	±0.05%	On flights 2112, 2217, 2417 257, and on the initial ascents of 239 and 247
100%	±0.15%	After initial ascents of flights 239 and 247
99%	±0.2%	All flights
98%	±0.4%	All flights
97%	±0.7%	All flights

Table 5. Estimated accuracies of RH measurements and effects of calibration changes during flights at SNI.

The accuracy of the hygrometer degraded in its use in the present cloud measurements as suggested by changes in the field calibrations done prior to and after each balloon flight. This first attempt at in-cloud measurements showed calibration changes owing to a misadjustment of the time response of the diode heaters. The adjustment was set too slow, which permitted the droplet deposit on the sensor to exceed the 100% value, and thus cause calibration changes. Table 5 gives the estimated accuracy for some of the flights. The time response of the sensor was approximately 3 s for all flights with the exception of flights 239 and 247; after the initial ascent of these two flights the time response was approximately 15 s. The calibration voltage VC, established at the surface air temperature, has a temperature coefficient of approximately 0.3% per °C. For example, if the air temperature during the flight has decreased by 10°C then VC must be decreased by 3%.

Under normal operating conditions $V3$ cannot exceed VC. However, if the sensor does not respond rapidly enough near RH = 100%, then $V3$ will exceed VC under conditions of supersaturation. This occurs, for example, on the ascent of flight 239. For this and other similar cases proceed as follows: subtract VC from $V3$, multiply the difference by 0.1% RH/0.125 V, and add the result to $V4$ which is the supersaturation percentage determined from channel 4 which is described next.

Saturation Hygrometer, $RH2$ (RH $\geq$ 100%)

This is the second channel of the instrument described in the previous section.

$$RH2 = V4 - VB2 \qquad (8)$$

where $V4$ is the output voltage stored in the data file OUTXXYY.SHR and

$VB2$ is the average background voltage, which must be determined from a plot of the data.

The algorithm in Eq.(8) applies to all flights except for 239 where $RH2$ must be divided by the factor 3, because for this flight this channel was run with three times the normal sensitivity.

Forward Scatter Meter, LWC (g/m^3)

This instrument is described in Gerber (1987). The instrument measures the near forward scattered light of particulates irradiated by a narrow beam of light from a HeNe laser. The scattered light can be shown to be strongly correlated to the far infrared extinction coefficient of those particulates, and

hence is proportional to the liquid water content according to the Chylek (1978) relationship. The measurement is in situ and has a response time faster than the 5 Hz sampling rate of the data logger.

$$LWC = \frac{0.084\text{g/m}^3}{V} (V5 - VB3) \qquad (9)$$

where *V5* is the output voltage stored in the data file OUTXXYY.FSM and

> *VB3* is the background voltage, which must be determined from a plot of the data during non cloud conditions.

Equation (9) holds for all flights except flights 1515, 1609, and 1617 for which the *LWC* values must be divided by the factor 2 since the instrument was adjusted to have twice the sensitivity. Examples of *LWC* are shown in Figs. 6 and 7 for 100-s periods during the ascent of the balloon on flight 239. Figure 6 shows a plot that gives correct values for *LWC*. Figure 7 shows a plot of *LWC* that is contaminated with RF noise from the LTA telemetry system. The spectrum of this noise is not known. For sections of the *V5* data file (OUTXXYY.FSM) containing the RF noise it is suggested that the *V5* data which was telemetered to the ground station and logged at 0.3 Hz, be used in place of the contaminated data. The telemetered *V5* data is stored in the data file LTAXXYY.

Bivane Anemometer Wind Speed, V_s (m/s)

The bivane is a Model No. 21003 from the R.M. Young Company. It was designed specifically for micrometeorological research. It is a low-inertia, fast-response, bidirectional wind vane that measures both the azimuth angle and the elevation angle of the wind. The wind speed sensor is of the propeller type whose dynamic response has been very carefully matched to the dynamic response of the vane.

$$V_s = 4.00 \ (V6 - 0.02 \ \text{V}),\tag{10}$$

where *V6* is the output voltage of the anemometer stored in the data

> file OUTXXYY.BAW.

Bivane Azimuth, α_v (deg.)

$$\alpha_v = (V7 - 2.77 \ \text{V}) \ \frac{70.4°}{\text{V}}\tag{11}$$

where *V7* is the output voltage of the anemometer stored in the data

> file OUTXXYY.BAA.

The bivane was lined up with the instrument-package compass, which is aligned to point upwind. A clockwise rotation from the compass direction gives positive values in Eq.(11), counterclockwise rotation from the compass gives negative values in Eq.(11).

Bivane Elevation, ϵ (deg.)

$$\epsilon = (V8 - 2.73 \ \text{V}) \ \frac{22.67°}{\text{V}},\tag{12}$$

11
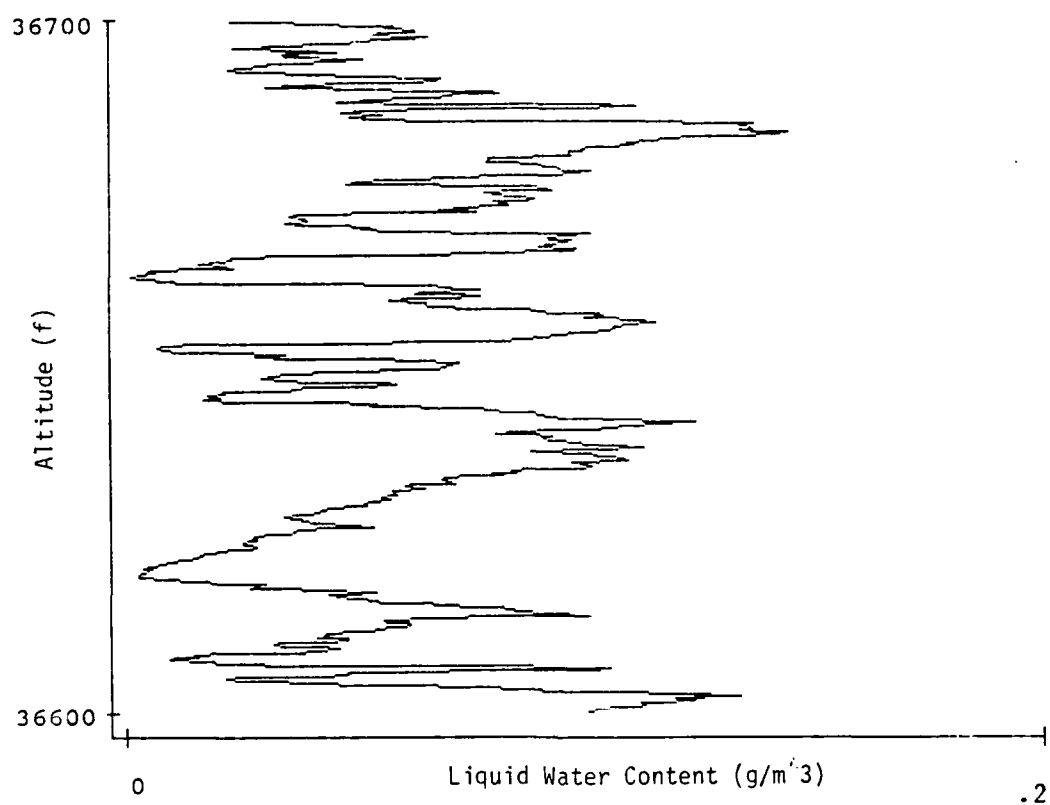
Fig. 6 Proper instrument signal (*V5*) converted to LWC for a 100 s
period during the ascent of flight 239.
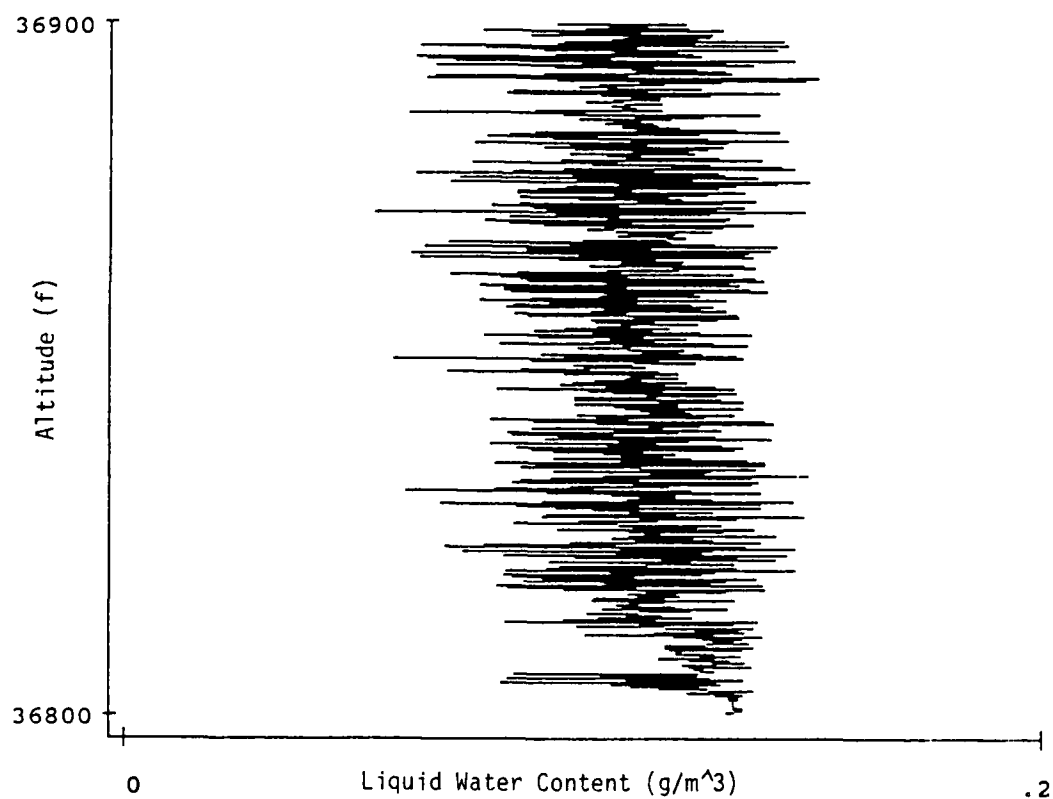
Fig. 7 Instrument signal (*V5*) converted to LWC showing RF noise
contamination.

12

where $V8$ is the output voltage of the anemometer stored in data file

OUTXXYY.BAE.

The elevation angle of the bivane is the deviation of the vaned anemometer of the instrument from the horizontal position. A positive value given by Eq.(12) indicates the bivane is pointing up (downdraft), and a negative value indicates that the bivane is pointing down (updraft).

Nephelometer, σ_s (1/Km)

This nephelometer is described in Gerber (1986). The instrument uses a Xenon flash filtered to obtain photopic response. The flash is triggered every 2 s and the scattering coefficient output consists of a stepwise signal refreshed every 2 s.

$$\sigma_s = (V9 - 0.107 \text{ V}) \frac{0.177 \text{ Km}^{-1}}{0.148 \text{ V}} \tag{13}$$

where $V9$ is the output voltage of the nephelometer stored in data file
OUTXXYY.NEP

Given that the scattering coefficient consists of light integrated over slightly less than π means that the value given by Eq.(13) will under estimate the true scattering coefficient when particles are large (such as in a cloud). A correction factor for this underestimate is given in Gerber (1986).

Ozone Meter

This new instrument was on loan from and operated by the University of Denver. The instrument failed to provide any useful data. The name of the data file is OUTXXYY.OZS.

Altimeter, h (m)

The altimeter is a Model 7000 from Computer Instruments Corp. The accuracy of the altimeter is $\pm$ 5 ft and the precision is $\pm$ 1 ft . The altimeter data is stored in several data files. See Appendix A for a listing of the data file names and what they contain. Table 6 contains a listing of the flight names and values for $V11_{min}$ which were used for the plots in Appendix C as well as a time difference that is referred to later.

$$h_b = 0.342 \, [V11 - (V11_{min} - 50)] \tag{14}$$

and

$$h = h_b - 38 \text{ m}, \tag{15}$$

where h_b is the height above sea level of the balloon,

       $V11$ is the altitude stored in the data files,

       $V11_{min}$ is the altitude indicated on the data files when the balloon begins its ascent, and

       h is the height above sea level of the instrument package.

13

Flight Name	Minumum Altitude	Time Difference
1515	1468	215.6
1609	1438	---
1617	1486	100.0
1710	1408	98.0
187	1358	101.0
1814	1366	103.2
195	1461	104.6
1913	1461	107.1
2008	1414	109.2
2017	1429	110.0
2112	1323	110.85
2217	1399	117.0
239	1389	118.45
2315	1417	118.45
247	1439	123.0
2417	1474	120.4
257	1477	124.0

Note: The time difference listed is a value which should be subtracted from the times stored in the data files with the LTAXXYY prefix to synch-ronize the time with that of the instrument package clock..

Table 6. Time difference between instrument package clock and the ground station clock as well as the minumum altitudes for each flight.
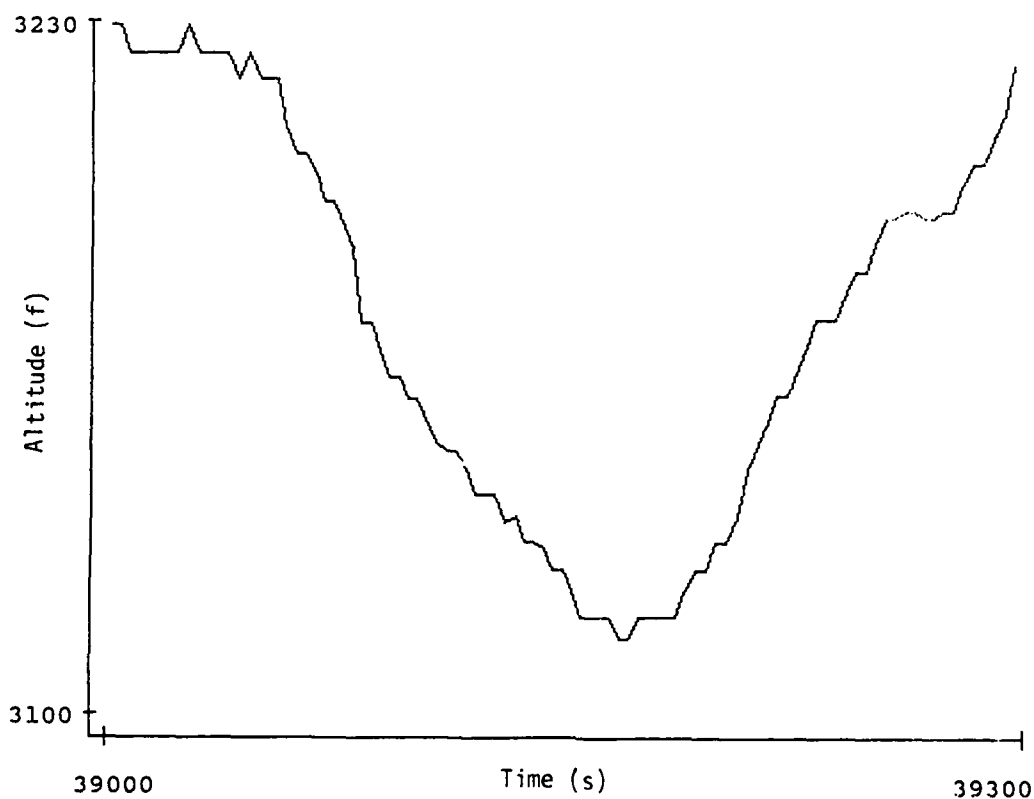
Fig. 8 Example of raw height-time data from the data file LTAXXYY. Data sampling rate was 0.3 Hz.

Because of RF noise from the telemetry system it was not possible to record altitude with the data logger on the instrument package. All height data must be obtained from the telemetered signal recorded by the ground station data logger. An example of a 300-s increment of the *V11* signal from LTAXXYY. is shown in Fig. 8 for flight 239. The curve in this figure shows the effects of the 0.3 Hz data rate and digitization noise. A 5 point running mean of the same data segment is shown in Fig. 9. This smoothing was found to be a good compromise between reducing noise in the height data and retaining height accuracy.

Particle Spectrometer, *dn/dlogr* [number of particles/μm, cm^3]

The particle spectrometer is a CSASP instrument from Particle Measuring Systems. The instrument belongs to and was operated by UMIST.

$$\frac{dn}{d \log r} = \frac{N}{F\, t_s\, (\log r_2 - \log r_1)}$$ (16)

where *N* is the particle count in each channel,

r is the particle radius in μm,

r_2 is the upper radius limit of channel i,

r_1 is the lower radius limit of channel i,

t_s is the sampling time

F is the flow rate of the instrument, 10.22 cm^3/s

The instrument was used with 15 channels in each of two size ranges.

Size range 0, 1 - 16 μm radius particles, $\Delta r = 1$ μm

Size range 1,0.5 - 8 μm radius particles, $\Delta r = .25$ μm

Table 7 shows an example of how *N*, t_s , and time of the particle measurements are stored in the data file OUTXXYY.MST. The time of the measurement is given first (e.g. 10: 9:36). The next line consists of two sets of 16 numbers. The first set is for size range 0 and the second set is for size range 1. The first number in each set is the value of t_s for each size range, divide by 100 to get t_s in seconds. The other 15 numbers in each set are values of *N* for each channel.

Clock, *t* (s)

Quartz clocks were used for both the instrument package data logger and the ground station data logger. The clocks were not synchronized, the clock in the instrument package data logger was ahead of the ground station data logger clock on all flights. Table 6 shows the difference between these two clocks for the 17 flights. This time should be subtracted from the times given in the files LTAXXYY. and LTAXXYY.SMO to synchronize them with the times in the data files with the OUTXXYY prefix. Time *t* is stored in several data files. See the description of data files in Appendix A for more information. The times given

15

Altitude (f)

3230

3100

39000   Time (s)   39300

Fig. 9 Data in figure 8 smoothed with a five point running average.

```
10: 9:43
50   80  163 15    5  1  1  0  0  0  0  0  0  0  0  0 42  159  233  242 156 83 75  79  69  56  26   5   5   2  0  3
10: 9:44
50  155  489 127  13  3  1  1  0  0  0  0  0  0  0  0 42  126  119  107  83 70 96 109 179 135  76  55  33  20 12  5
10: 9:45
50  121  441 276  63 16  4  1  1  0  0  0  0  1  0  0 47  112   66   48  38 39 35  64  75  90  73  53  60  61 28 20
10: 9:46
50   93  438 410  83 20  5  0  3  2  0  1  0  1  0  0 42  114   48   50  30 34 34  54  77  76  98  77  84  69 66 34
10: 9:47
50  171  625 489  88 22  3  3  2  1  0  0  1  0  0  0 42  141   52   33  28 39 56  96 144 173 118 142 107  95 59 36
10: 9:48
50  146  628 573  93 21  9  3  2  1  0  0  0  0  0  0 42  133   46   29  30 22 40  81  94 108 137 118 127 119 70 31
10: 9:49
50  179  628 571  85 25  5  2  1  0  0  0  0  0  0  1 42  147   43   42  33 24 50  66 116 109 125 125 154 120 63 34
10: 9:50
50  115  543 431  93 18  5  1  3  1  0  1  0  0  0  0 47  172   61   51  40 24 59  88 128 153 103 130 126  74 57 41
10: 9:51
50   86  335 277 110 27  5  6  5  1  2  1  2  0  0  0 42  122   77   71  39 29 47  68 116  86  67  55  61  51 42 29
10: 9:52
50   54  235 288 169 55 17  6  2  0  0  2  3  1  0  0 42  142   71   82  40 24 24  29  43  42  51  60  62  61 33 49
10: 9:53
50   56  268 287 165 44 12  4  1  2  2  1  6  1  0  1 42  123   61   61  26 17 25  42  51  48  47  58  67  69 55 35
10: 9:54
50   79  258 318 128 47 18  5  2  2  4  1  2  1  3  0 42  132   50   43  31 25 26  42  43  49  70  59 57   61 53 38
10: 9:55
50   41  204 316 165 44 16  4  3  2  0  2  2  1  0  0 47  129   76   81  28 19 23  24  37  56  51  60 72   67 58 55
10: 9:56
50   39  180 289 150 36 12  5  4  2  0  1  0  0  1  0 42  111   74   76  23 15 12  25  34  35  34  57 49   36 45 27
```

Note: Several spaces have been removed between the numbers in this table to allow the printout to fit on this page. The data file OUTXXYY.MST contains lines which are approximately twice the length of those shown.

Table 7. Example of the CSASP particle spectrometer data stored in the file OUTXXYY.MST.

16

in the data files OUTXXYY.MST and LTAXXYY. are given in the form hours, min-
utes, seconds; in all other files t has been converted to seconds.

Support Line Compass, α_i (deg.)

This compass is a flux-gate magnetometer, Model NO. 930-555/1 from Marinex
Inc., MA. Its accuracy is $\pm$ 1°, and response time is 1 s.

For $V14$ < 0.33 V,

$$\alpha_i = 225°; \tag{17}$$

for 0.33 V $\leq$ $V14$ $\leq$ 2.34 V,

$$\alpha_i = 45° + \cos^{-1}\left(\frac{V14 - 3.905 \text{ V}}{1.005}\right) \tag{18}$$

for 2.34 V < $V14$ $\leq$ 2.54 V

$$\alpha_i = 45° \tag{19}$$

for 2.54 V < $V14$ < 2.74 V

$$\alpha_i = 225° \tag{20}$$

for 2.74 V $\leq$ $V14$ $\leq$ 5.07 V

$$\alpha_i = 405° - \cos^{-1}\left(\frac{V14 - 3.905}{1.165}\right) \tag{21}$$

for $V14$ > 5.07

$$\alpha_i = 45° \tag{22}$$

where $V14$ is the output voltage stored in the data file OUTXXYY.SLC.

If the preceding algorithms predict α_i > 360° , then subtract 360° from α_i.

Pallet Compass, α_p (deg.)

This compass is the same type as the support line compass that was des-
cribed previously.

For $V15$ < 0.26 V

$$\alpha_p = 225°; \tag{23}$$

for 0.26 V $\leq$ $V15$ $\leq$ 2.39 V

$$\alpha_p = 45° + \cos^{-1}\left(\frac{V15 - 1.325 \text{ V}}{1.065}\right); \tag{24}$$

for 2.39 V $<$ $V15$ $\le$ 2.58 V,

$$\alpha_p = 45°; \tag{25}$$

for 2.58 V $<$ $V15$ $<$ 2.77 V,

$$\alpha_p = 225°; \tag{26}$$

for 2.77 V $\le$ $V15$ $\le$ 5.12 V,

$$\alpha_p = 405° - \cos^{-1}\left(\frac{V15 - 3.945}{1.175}\right); \tag{27}$$

and for $V15$ $>$ 5.12 V

$$\alpha_p = 45° \tag{28}$$

where $V15$ is the output voltage stored in data file OUTXXYY.PAC.

If the preceding algorithms predict that α_p $>$ 360° , then subtract 360° from α_p.

Support Line Inclinometer #1, θ_1 (deg)

The inclinometer is the Accustar Model from Sperry Corporation, Pheonix, AZ. The precision of the instrument is 0.001°, the linearity is 0.1° and the time response is 1 s.

$$\theta_1 = \frac{V16 - 4.81 \text{ V}}{0.060 \text{ V/deg}} \tag{29}$$

where $V16$ is the output voltage stored in data file OUTXXYY.IN1.
This inclinometer was lined up with the direction mark on the support line compass. For nadir, the output of the inclinometer is 0°. A clockwise rotation gives a negative output and a counterclockwise rotation gives a positive output.

Support Line Inclinometer #2, θ_2 (deg)

This is the same type of inclinometer described previously.

$$\theta_2 = \frac{V17 - 5.16 \text{ V}}{0.060 \text{ V/deg}} \tag{30}$$

where $V17$ is the output voltage stored in data file OUTXXYY.IN2.

This inclinometer was mounted perpendicular to inclinometer #1. A clockwise rotation from nadir of inclinometer #2 gives positive values in Eq.(30) and a counter-clockwise rotation gives negative values in Eq.(30).

Telemetry System

This telemetry system is owned and was operated by LTA, Inc. Several channels of data were telemetered to the NRL ground station and logged at approximately 0.3 Hz. The data, which were telemetered are stored in the data file LTAXXYY. Table 8 shows an example of the format of this data file. Among the data telemetered to the NRL ground station was the fsm, dry bulb-wet bulb, altitude and time.

Video Camera

The video camera was on loan from Colorado State University. The camera was attached to the instrument package so that it pointed into the wind. After flight 239 the window on the camera enclosure had become contaminated causing a loss of nearly all visual information.

DATA REDUCTION

The data obtained during the experiment has been converted from a binary format to ASCII, with each channel of data being stored in a separate file for each flight. There are nineteen data files for each flight, excluding flight 1609 in which all of the data stored on the instrument package was inadvertently lost. Two files have been created for each flight that contain time and altitude data for both the 1 Hz and 5 Hz data. These files are of the same length as there corresponding data files. There are nine data files that contain 5 Hz data and eight data files that contain the 1 Hz data for each flight. Two files contain the data telemetered to the ground station that was recorded at approximately 0.3 Hz.

The 5 Hz data files are arranged in sequential order and each line of data in the data files corresponds to a line of data in the 5 Hz time and altitude data files. Table 9 shows the way in which the data in the time and altitude files corresponds to that in the data files. The above correlation is true for the 1 Hz data files and the 1 Hz time and altitude files.

The data files have been compressed by using a program called PKARC Version 3.3 which is an archiving program. Once the data files for a flight have been compressed, the data for the whole flight can be stored on a single 1.2M floppy disk for all but a few of the longer flights, which use approximately 1.8 MB of disk space. Table 10 lists the archived data files for flight 239 showing the original size and the size after compression of each data file. These "crunched" data files can be converted back to the ASCII form by using the program PKXARC Version 3.3. Once reconverted to ASCII, each data file takes up about 900 KB of disk space. Appendix B describes the commands of PKARC and PKXARC.

DATA QUALITY

Use of the data requires careful attention to its quality because not all instruments were operating properly for all of the flights. As stated previously, some of the measurements were contaminated with RF noise generated by the LTA telemetry system. The FSM, dry-wet bulb temperature, and altimeter were all affected by this noise at certain times during several flights. The forward-scatter meter was overranging on the first several flights. During flight 1710 heavy drizzle in the clouds caused the saturation hygrometer to

Hour	Minute	Sec	Sec/100		Dry-Wet Bulb	FSM		Altitude	
9	45	10	51	94628	1.34	0.42	35.8	1398	0
9	45	13	42	94631	1.35	0.38	35.8	1398	0
9	45	16	66	94634	1.35	0.42	35.8	1398	0
9	45	19	52	94637	1.34	0.38	35.8	1389	0
9	45	22	60	94640	1.35	0.41	35.8	1389	0
9	45	25	78	94643	1.34	0.42	35.8	1389	0
9	45	28	64	94646	1.34	0.42	35.8	1389	0
9	45	31	71	94649	1.35	0.4	35.8	1389	0
9	45	34	90	94652	1.35	0.39	35.8	1389	0
9	45	37	76	94655	1.34	0.42	35.8	1398	0
9	45	41	0	94658	1.34	0.39	35.8	1398	0

Table 8. Example of the data file LTAXXYY. which contains the data telemetered to the NRL ground station.

Line Number	Data File OUTXXYY.TAL		Data File OUTXXYY.FSM
	TIME	ALTITUDE	FSM
Line 1	36020.0	1433.21	0.433
Line 2	36020.2	1433.26	0.431
Line 3	36020.4	1434.00	0.432
.	.	.	.
.	.	.	.
.	.	.	.
Line n-1	39364.6	1431.00	0.433
Line n	39364.8	1430.00	0.444
	EOF	EOF	EOF

(EOF = End Of File)

Table 9. Example of how the data files are related to one another.

Filename	Original Length	Compression Method	Compressed Length	Ratio
LTA239	151099	Crunched	43623	72%
LTA239.SMO	54936	Crunched	21435	61%
OUT239.BAA	884336	Crunched	76656	92%
OUT239.BAE	884336	Crunched	84081	91%
OUT239.BAW	884336	Crunched	96333	90%
OUT239.FSM	884336	Crunched	92279	90%
OUT239.IN1	176852	Crunched	18236	90%
OUT239.IN2	176852	Crunched	18683	90%
OUT239.MST	1711462	Crunched	245769	86%
OUT239.NEP	176852	Crunched	21633	88%
OUT239.OZS	176852	Crunched	15317	92%
OUT239.PAC	176852	Crunched	17224	91%
OUT239.PDB	884336	Crunched	82762	91%
OUT239.PDT	884336	Crunched	92417	90%
OUT239.SHI	884336	Crunched	83379	91%
OUT239.SHR	884336	Crunched	21542	98%
OUT239.SLC	176852	Crunched	20537	89%
OUT239.TAL	1675584	Crunched	409914	76%
OUT239.TAS	335088	Crunched	83536	76%

Table 10. Listing of archived data files for flight 239 showing file size before and after "Crunching".

fail and during some of the other flights a drift in the sensor was noticed; however, useful data was collected. Only a limited record was obtained with the video camera, the best during flight 239 while flying above cloud top. Cloud droplets and condensation collecting on the window of the camera enclosure produced poor results while in cloud. The CSASP particle spectrometer and other sensors functioned properly throughout the experiment.

RESULTS

The analysis of this data set has just begun, therefore very few results are presently available. Figures 10 and 11 give examples of LWC and RH as measured by the forward-scatter meter and the saturation hygrometer, respectively. Both profiles are for the ascent of flight 239 when a fractional cloud cover of strato-cumulus was in the process of dissipating. Figure 10 shows the cloud layer extended from 500 to 650 m, and that the LWC profile was very different from the adiabatic LWC profile. Figure 11 shows that RH within the cloudy air ranges from about 99.5% to 100.2%, and that deep layers of subsiding air exist in the clouds where RH < 100%. The large subsaturated and supersaturated conditions suggested by Curry (1986) for Arctic stratus were not seen in the marine strato-cumulus. In Fig.11 the supersaturation peak at the top of the main cloud at 625 m is consistent with radiation-forcing calculations of Davies (1985); although, the cause of the peak owing to a strong updraft cannot be ruled out until the w field is analyzed.

INTERPRETATION OF BIVANE WIND MEASUREMENTS

The bivane anemometer on the instrument package measures the wind velocity V" in a Cartesian coordinate system referenced to the flat surface of the instrument package and to the direction in which the instrument package points, see Fig.12. The desired information are the u, v and w components of the wind velocity V, in the Cartesian coordinate system fixed to the Earth's horizontal surface. Because of forces exerted on the instrument package by the motion of the balloon and by the wind, the plane of the instrument package moves through various positions so that the coordinate systems of the instrument package and the Earth generally do not coincide. The problem consists of transforming V" to V.

The following motions of the instrument package must be considered: The yaw, pitch, and roll of the instrument package changes as a function of time, thus an orthogonal transformation from the V" to the V coordinate systems is necessary, and the velocity owing to the motion of the instrument package must be subtracted. In addition, the horizontal and vertical motions of the balloon must be taken into account.

Known Quantities and Degrees of Freedom

The wind vector V" is given from the measurements of the bivane anemometer wind speed V_s, azimuth α_v, and elevation ϵ.

The position in space of the pallet is estimated from the measurements of the support line inclination θ, the support line azimuth α_s, the instrument package azimuth α_p, and the altimeter h.
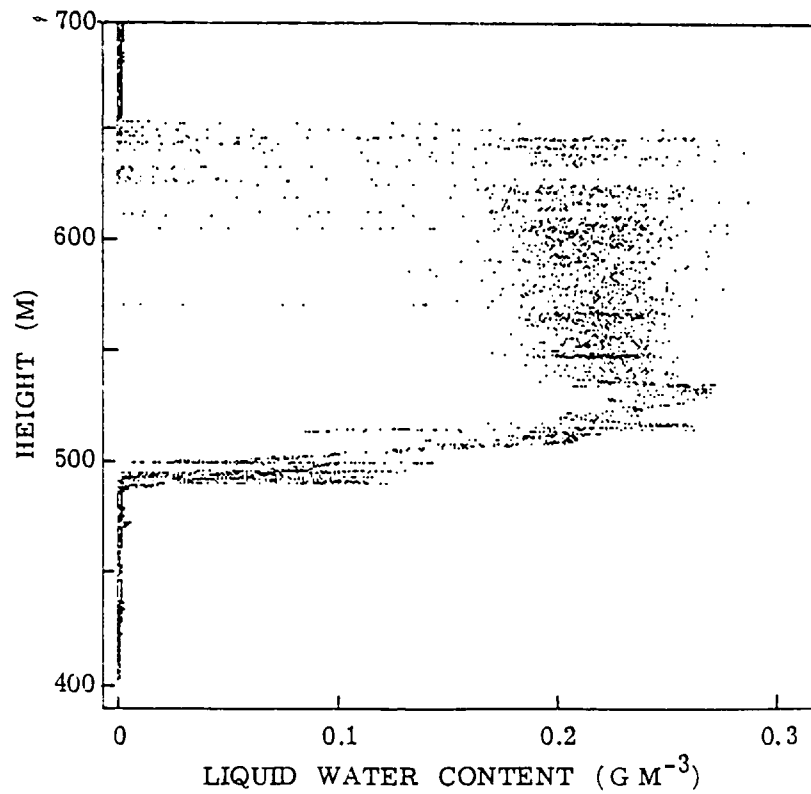
Fig.10 Liquid water content on the ascent of flight 239 during
strato-cumulus dissipation.
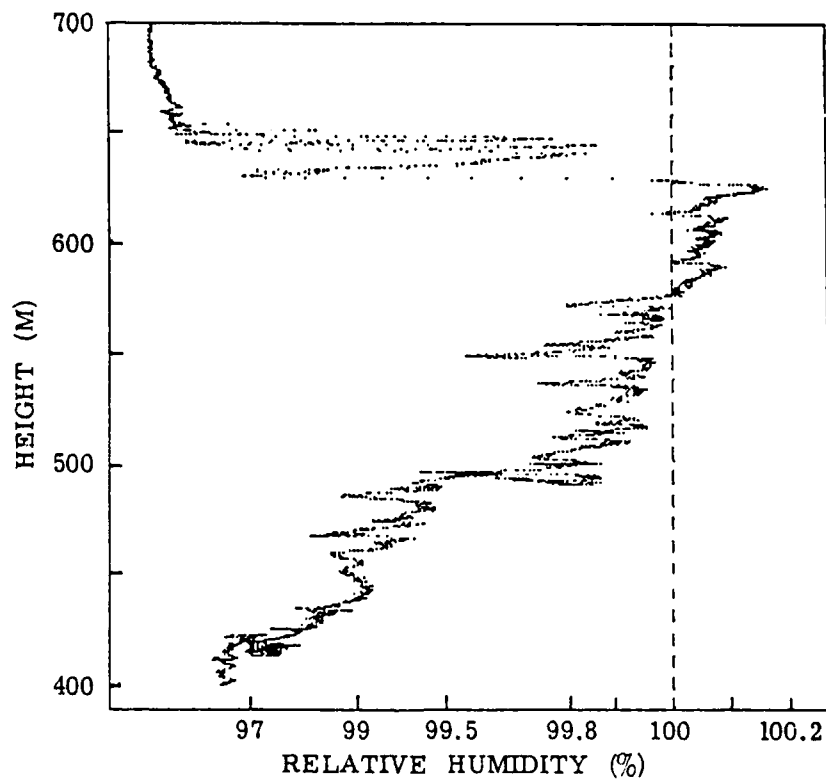
Fig.11 Relative humidity profile measured with the saturation hygrometer
on the ascent of flight 239.
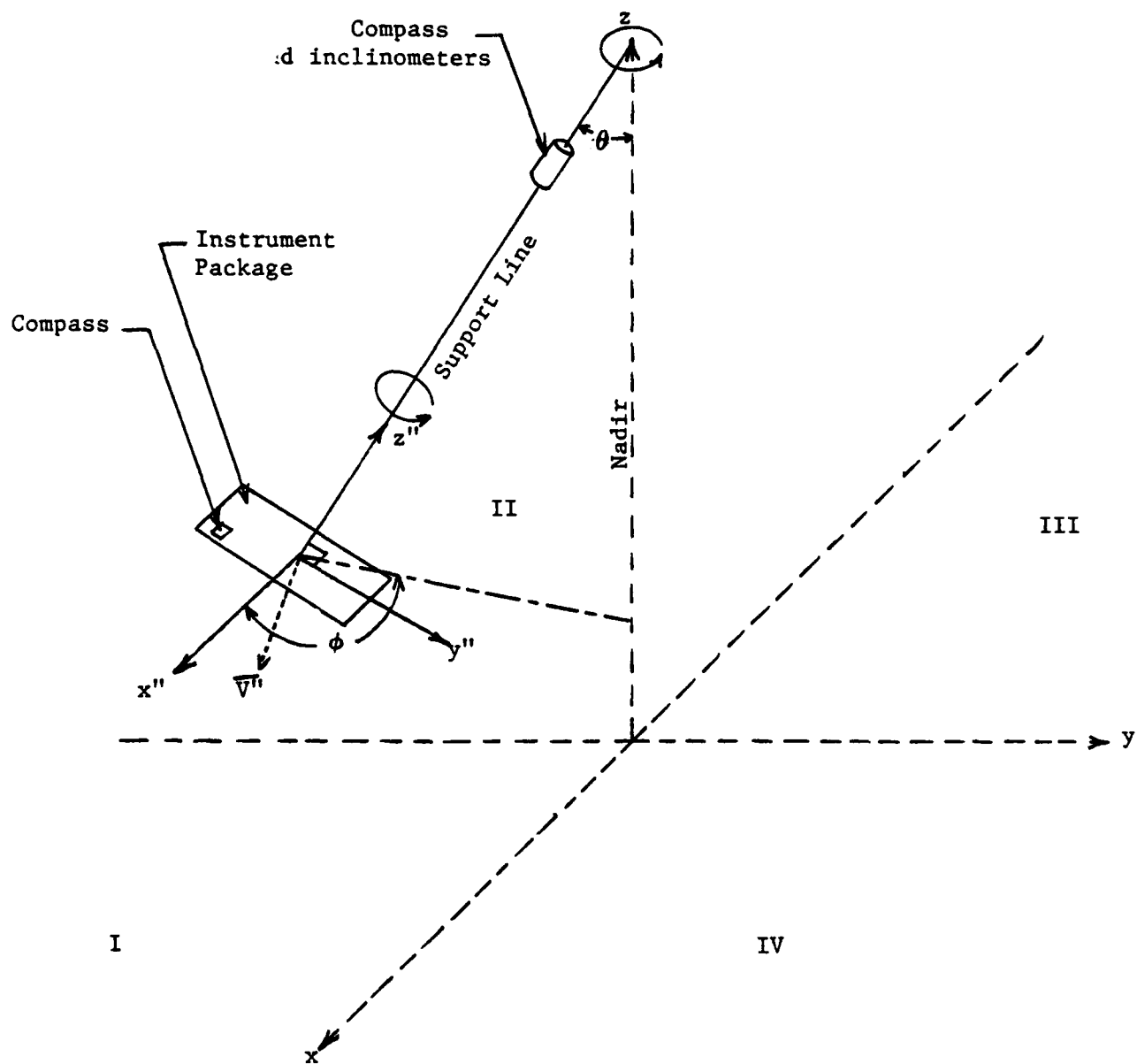
Fig.12 Coordinate systems of instrument package and Earth.

The degrees of freedom for the motion of the pallet consist of variable θ, α_s , and ϕ (the difference between α_s and α_p), horizontal motion of the balloon and the vertical motion of the balloon.

Assumptions

To utilize the typical analytical transformation of V'' to V, as is done for aircraft turbulence measurements, requires precise measurements of the position of the V'' coordinate system in space as a function of time. These measurements are usually accomplished using an inertial platform which gives precise accelerations in 3 dimensions. The system of position sensors on the instrument package and the balloon are not capable of such precise position- ing; however, by establishing reasonable assumptions for the motions and ge- ometry of the balloon/instrument package combination, the available sensors permit a transformation which gives useful information on u, v, and w.

The assumptions are as follows:

A. The angle between the support line and the instrument package remains constant at the instrument package, as suggested by the observed motion of the instrument package.

B. The observed pendulum-type motion of the instrument package (period of about 11.8 s) below the balloon is primarily in the z-y plane, which is per- pendicular to the wind direction x. This means that the value of the pallet azimuth α_p will remain essentially unchanged during the coordinate system transformation.

C. Only the vertical motion of the balloon is considered as affecting V''. The 1 Hz data of the positioning devices is not fast enough to include the horizontal motion of the balloon, which could otherwise be established by it's affect on the motion of the instrument package. This assumption affects values of v, and to a much lesser degree u and w.

D. Because of wind pressure on the instrument package and on the support line, the instrument package experienced slight blowback, which consists of a mean support line inclination that deviates from nadir in the downwind direc- tion. Under blowback conditions the support line does not describe a straight line. but is inclined at a greater angle at the location of the inclinometers at the top of the support line than at the instrument package. An algorithm can be established to relate the inclinometer measurements at the top of the support line to the inclinations of the line at the pallet.

Approach

The procedure for transforming V'' to V is as follows.
A. The blowback algorithm for correcting the inclinometer measurements is established first. This is done by transforming V'' to V after the vertical motion of the balloon is subtracted, and then comparing the mean bivane ele- vation to the mean inclinometer readings for various mean wind speeds.

B. u v, and w are determined by transforming V'' to V, subtracting the horizontal and vertical velocity of the instrument package as determined by the instrument package's trajectory in the x-y plane, and subtracting the ver- tical motion of the balloon.

24

Coordinate Transformation

An orthogonal transformation between the Cartesian coordinate systems for **V"** and **V** is desired. The coordinates of the velocity vectors can be related by

$$x = \alpha_{11}x" + \alpha_{12}y" + \alpha_{13}z", \tag{31}$$

$$y = \alpha_{21}x" + \alpha_{22}y" + \alpha_{23}z", \tag{32}$$

and

$$z = \alpha_{31}x" + \alpha_{32}y" + \alpha_{33}z", \tag{33}$$

where α_{ij} are coefficients which are functions of the Eulerian angles of rotation (for additional clarification see for example a text such as <u>Classical</u> <u>Mechanics</u> by H. Goldstein, 1950).

Two such rotations of the axes (see Fig.13), which take into account the pitch and roll of the instrument package, are used to convert x", y", and z" to x, y, and z under the assumption that both x" and x are lined up with the instrument package compass. The difference between the x" and x directions is small, because θ varies by no more than about $\pm 10°$, and the motion of the instrument package is primarily perpendicular to the wind direction. Following the transformation of **V"** to **V**, the yaw of the instrument package caused by its motion is compensated for by subtracting the instrument package's velocity as determined from the inclinometers from **V**. The pendulum motion of the instrument package requires that the vertical component of this motion also be subtracted from w.

The transformation is given by

$$\overline{x} = \overline{A}\,\overline{x}", \tag{34}$$

where $\overline{x}"$ and $\overline{x}$ are column matrices, and $\overline{A}$ is the complete transformation matrix.

Elements of $\overline{A}$ can be obtained by writing a double product of the transformation matrix for each rotation:

$$\overline{A} = \overline{B}\,\overline{C}, \tag{35}$$

where the initial counterclockwise rotation about x" defines $\overline{B}$:

$$\overline{x} = \overline{B}\,\overline{x}" \tag{36}$$

where

$$\overline{x}' = \begin{bmatrix} x' \\ y' \\ z' \end{bmatrix} \tag{37}$$

25
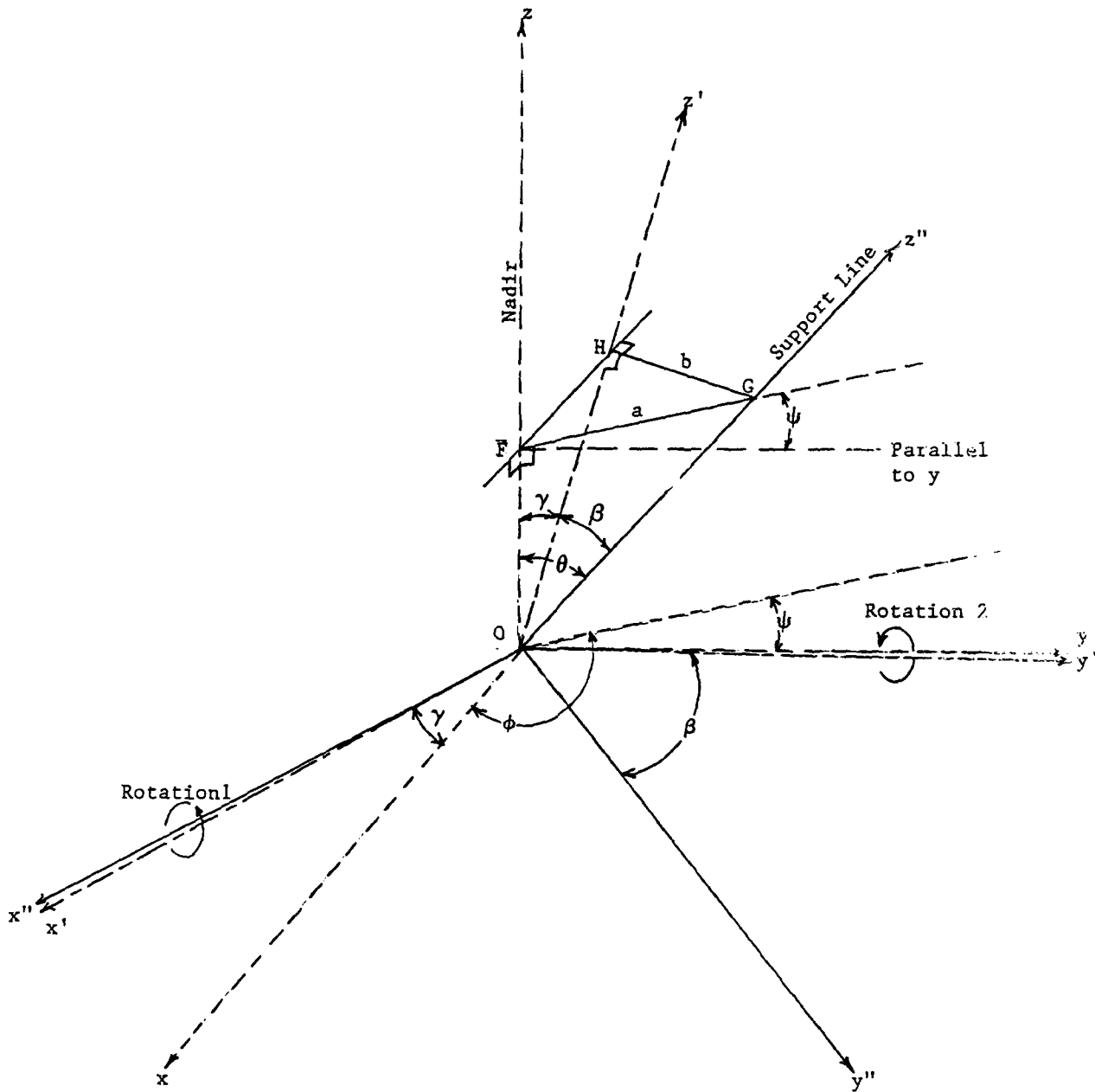
Fig.13 Double rotation of Cartesian coordinate system of instrument
package to that of Earth.

$$\bar{x}'' = \begin{bmatrix} x'' \\ y'' \\ z'' \end{bmatrix} \tag{38}$$

$$\bar{B} = \begin{bmatrix} 1 & 0 & 0 \\ 0 & \cos\beta & \sin\beta \\ 0 & -\sin\beta & \cos\beta \end{bmatrix} \tag{39}$$

Likewise, for the second counterclockwise rotation about y' or y gives

$$\bar{x} = \bar{C}\,\bar{x}' \tag{40}$$

or

$$\begin{bmatrix} x \\ y \\ z \end{bmatrix} = \begin{bmatrix} \cos\gamma & 0 & \sin\gamma \\ 0 & 1 & 0 \\ -\sin\gamma & 0 & \cos\gamma \end{bmatrix} \begin{bmatrix} x' \\ y' \\ z' \end{bmatrix}. \tag{41}$$

Therefore, from Eq.(35)

$$\bar{A} = \bar{B}\,\bar{C} = \begin{bmatrix} 1 & 0 & 0 \\ 0 & \cos\beta & \sin\beta \\ 0 & -\sin\beta & \cos\beta \end{bmatrix} \begin{bmatrix} \cos\gamma & 0 & \sin\gamma \\ 0 & 1 & 0 \\ -\sin\gamma & 0 & \cos\gamma \end{bmatrix} \tag{42}$$

which upon multiplying the matrices results in,

$$\bar{A} = \begin{bmatrix} \cos\gamma & 0 & \sin\gamma \\ -\sin\beta\,\sin\gamma & \cos\beta & \sin\beta\,\cos\gamma \\ -\sin\gamma\,\cos\beta & -\sin\beta & \cos\beta\,\cos\gamma \end{bmatrix} \tag{43}$$

The described result from Eqs.(34) and (43) is thus

$$\begin{bmatrix} x \\ y \\ z \end{bmatrix} = \bar{A} \begin{bmatrix} x'' \\ y'' \\ z'' \end{bmatrix}, \tag{44}$$

or

$$x = x''\cos\gamma + z''\sin\gamma$$

$$y = -x''\sin\beta \, \sin\gamma + y''\cos\beta + z''\sin\beta \, \cos\gamma \qquad (45)$$

$$z = -x''\cos\beta \, \sin\gamma - y''\sin\beta + z''\cos\beta \, \cos\gamma$$

The coefficients of x", y", and z" in Eq.(45) are given in terms of the Eulerian angles γ and β. It is necessary to find expressions for those angles in terms of the measured angles θ and ϕ.

From triangle FGH shown in Fig.13

$$z'' = z \cos\theta \qquad (46)$$

$$z'' = z'\cos\gamma \qquad (47)$$

and

$$z' = z \cos\beta \qquad (48)$$

where z, z', and z" are defined here as the coordinates where the triangle intersects the corresponding three axes.

Thus

$$z'' = z \cos\beta \, \cos\gamma = z \cos\theta \qquad (49)$$

and one of the desired relationships is found to be

$$\cos\theta = \cos\beta \, \cos\gamma \qquad (50)$$

A second equation is needed for relating ϕ to the other angles by using the previous figure and a top view of the triangle FGH shown in Fig.14, we find

$$a = z \sin\theta, \qquad (51)$$

$$b = z \sin\beta, \text{ and} \qquad (52)$$

$$b = a \cos\psi \qquad (53)$$

or

$$\cos\psi = \frac{\sin\beta}{\sin\theta}. \qquad (54)$$

However

$$\psi = \phi - 90° \qquad (55)$$

and

$$\cos\psi = \cos(\phi - 90°) = \cos(90° - \phi) = \sin\phi \qquad (56)$$

so that the desired expression is

$$\sin\phi = \frac{\sin\beta}{\sin\psi}. \qquad (57)$$

28
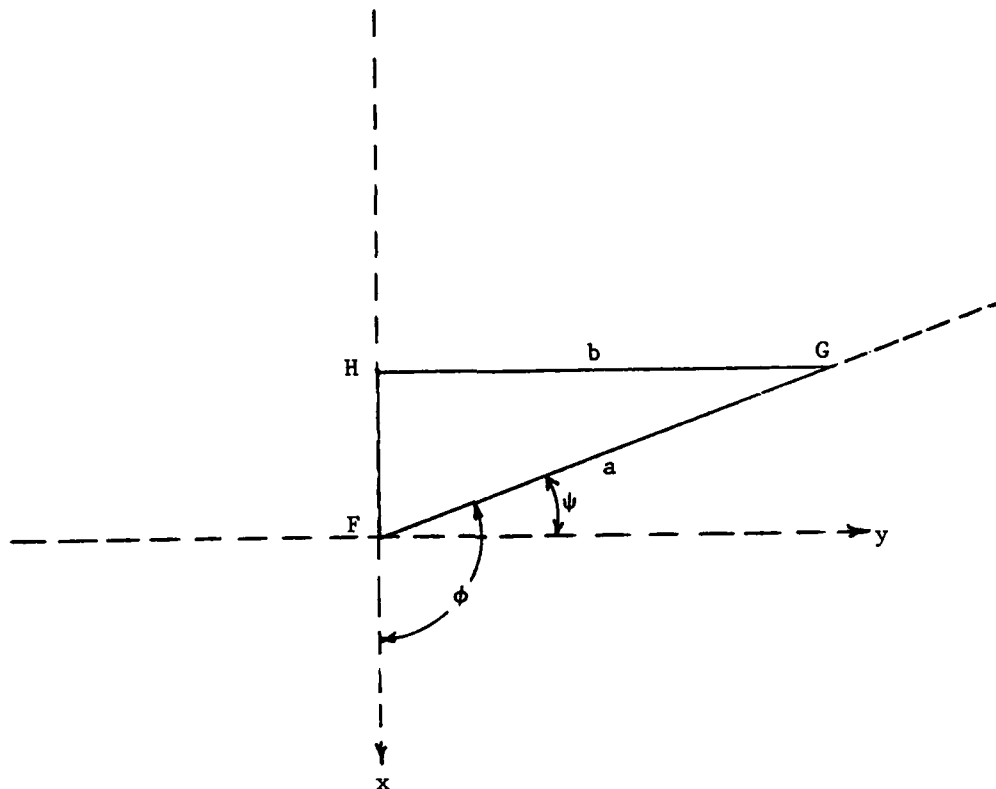
Fig.14 Top view of triangle FGH shown in figure 13.

Quadrant	Inclinometer #1	Inclinometer #2
I	−	+
II	+	+
III	+	−
IV	−	−

Table 11. The sign of the inclinometers in the various quadrants as shown in Figure 15.

Equations (45), (50), and (57) are sufficient to define **V** in terms of the measured quantities in the x", y", and z" coordinate system.

Support Line Inclination θ and Azimuth α_s

The support line inclination θ, needed in Eqs. (50) and (57), is a function of the measured values of θ_1 and θ_2 (see Fig.15) and is given by

$$\theta = \tan^{-1}(\tan^2\theta_1 + \tan^2\theta_2)^{\frac{1}{2}} \tag{58}$$

The angle ϕ, needed in Eq. (57), is the difference between the instrument package azimuth α_p and the support line azimuth α_s; as is determined as a function of α_i, θ_1, and θ_2 as follows: Given a Cartesian coordinate system referenced to nadir and the azimuth of the support line compass as shown in Fig.15, the sign of the inclinometer outputs places the support line in the proper quadrant in Fig.15 as given in Table 11.

The expression for α_s for each of the quadrants is

For Quadrant I

$$\alpha_s = \alpha_i + \tan^{-1}\left|\frac{y}{x}\right|; \tag{59}$$

for Quadrant II

$$\alpha_s = \alpha_i + 90° + \tan^{-1}\left|\frac{x}{y}\right|; \tag{60}$$

for Quadrant III

$$\alpha_s = \alpha_i + 180° + \tan^{-1}\left|\frac{y}{x}\right|; \tag{61}$$

and for Quadrant IV

$$\alpha_s = \alpha_i + 270° + \tan^{-1}\left|\frac{x}{y}\right|; \tag{62}$$

where

$$x = \tan\theta_1, \tag{63}$$

and

$$y = \tan\theta_2, \tag{64}$$

In using Eqs. (59)-(62), a conditional statement must be included: If $\alpha_s > 360°$, then subtract 360° from α_s.

It should be emphasized that α_p and α_s are compass directions that increase in the clockwise direction. This is contrary to the trigonometric convention where angles increase in the counterclockwise direction; ϕ is a trigonometric angle.

30
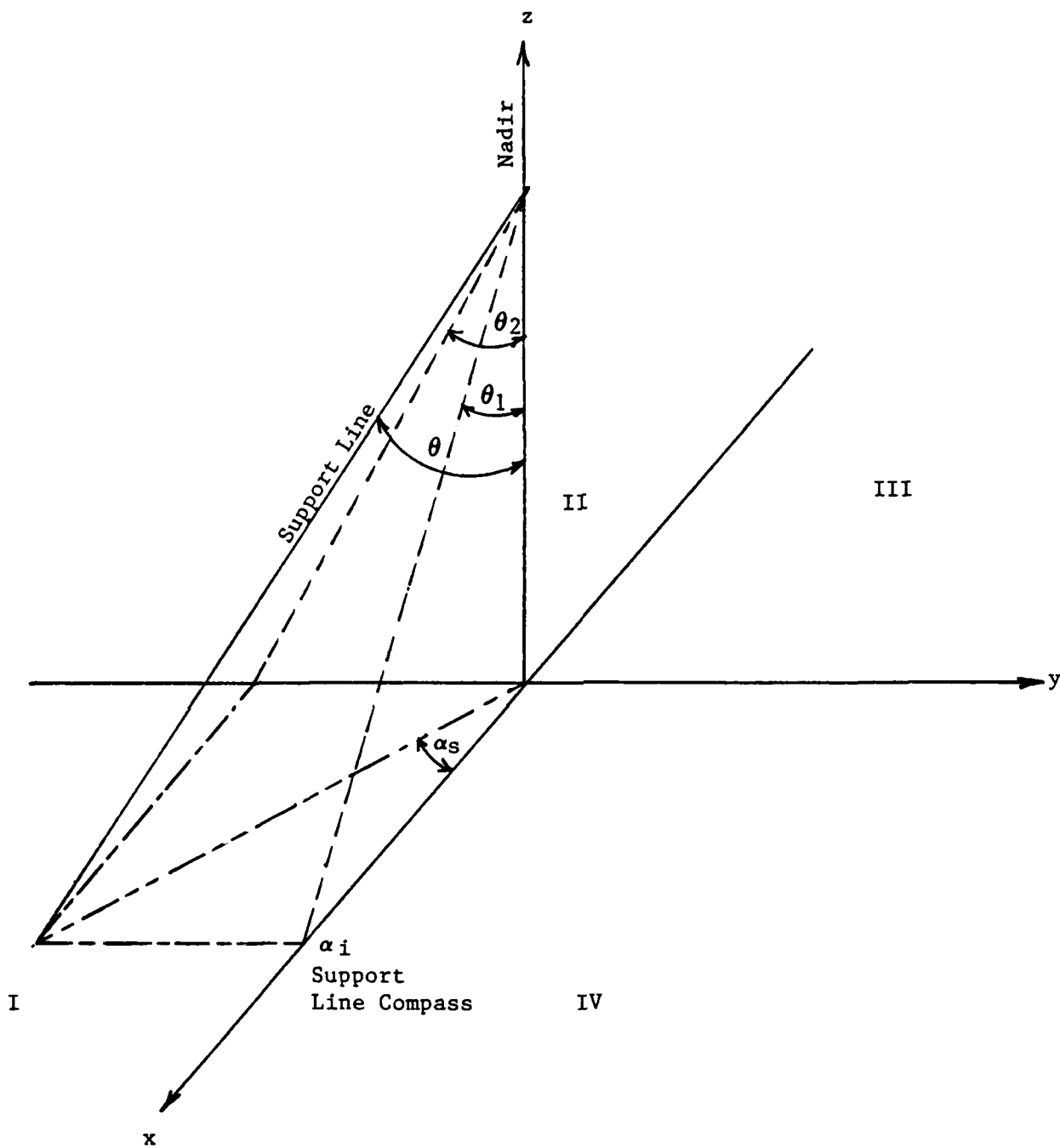
Fig. 15 Relationship of inclinometer measurements θ_1 and θ_2 to the support line compass direction α_p and support line azimuth α_s.

SUMMARY

This data set will make possible the first evaluation of the Navy's aerosol model NOVAM and will provide a better look at the clear and cloud topped boundary layer.

For the first time accurate RH measurements near 100% have been made in a cloud. These measurements were made in conjunction with other micro-physical measurements such as aerosol and cloud droplet spectra, and perhaps most important of all, they were all collocated with bivane turbulence measurements thus permitting flux calculations. The analysis of this data set, which consists of about 50% strato-cumulus cases including increasing and decreasing partial cloud cover, should lead to new insights on the physical mechanisms that drive the boundary-layer/cloud/turbulence system.

Addressing the entrainment mechanism at the top of the clouds should be especially amenable with this data set.

ACKNOWLEDGEMENTS

REFERENCES

Curry, J.A., 1986: Interaction among turbulence, radiation, and microphysics in Arctic stratus clouds, J. Atmos. Sci. 43, 90-106.

Chylek, P., 1978: Extinction and liquid water content of fogs and clouds, J. Atmos. Sci. 35, 296.

Davies, R., 1985: Response of cloud super saturation to radiative forcing, J. Atmos. Sci. 42, 2820-2825.

Gathman, S.G., 1989: A preliminary description of NOVAM, To be released in the near future.

Gerber, H., 1980: A saturation hygrometer for the measurement of relative humidity between 95% and 105%, J. Appl. Meteoro. 19, 1196-1208.

Gerber, H., 1986: Tethered balloon measurements at San Nicolas Island (Oct.1984): Instrumentation data summary, preliminary data interpretation, NRL Report 8972, 77 pp.

Gerber, H., 1987: Forward-scatter meter for estimating 10.6-um aerosol extinction, Applied Optics 26, 539-544.

Goldstein, H., 1950: Classical Mechanics, Library of Congress Catalog Number 50-7669.

APPENDIX A

DESCRPITION OF DATA FILES

The following table gives the names of all the data files obtained during the FIRE strato-cumulus experiment and a description of each file and the rates at which they were recorded.

File Name	Description	Sampling Rate
LTAXXYY.	Original LTA data. (Time, T, FSM, Altitude)	0.3 Hz
LTAXXYY.SMO	Smoothed LTA time and altitude.	0.3 Hz
OUTXXYY.BAA	Azimuth data.	5.0 Hz
OUTXXYY.BAE	Elevation data.	5.0 Hz
OUTXXYY.BAW	Wind speed data.	5.0 Hz
OUTXXYY.FSM	Forward scatter meter data.	5.0 Hz
OUTXXYY.IN1	Inclinometer #1 data.	1.0 Hz
OUTXXYY.IN2	Inclinometer #2 data.	1.0 Hz
OUTXXYY.MST	Particle spectrometer data.	1.0 Hz
OUTXXYY.NEP	Nephelometer data.	1.0 Hz
OUTXXYY.OZS	Ozone meter data.	1.0 Hz
OUTXXYY.PAC	Pallet compass data.	1.0 Hz
OUTXXYY.PDB	Psychrometer dry bulb data.	5.0 Hz
OUTXXYY.PDT	Psychrometer dry-wet bulb data.	5.0 Hz
OUTXXYY.SHI	Saturation hygrometer RH<100%	5.0 Hz
OUTXXYY.SHR	Saturation hygrometer RH>100%	5.0 Hz
OUTXXYY.SLC	Support line compass data.	1.0 Hz
OUTXXYY.TAL	Time and altitude data.	5.0 Hz
OUTXXYY.TAS	Time and altitude data.	1.0 Hz

APPENDIX B

DESCRIPTION OF COMPRESSION PROGRAM PKARC

This appendix gives a description of the commands used when running the program PKARC and PKXARC. Because of the massive size of the data files it was necesary to compress the data files for each flight to a reasonable size for purposes of storing and transferring the data. Compression ratios of 90% are not uncommon with PKARC.

INSTRUCTIONS FOR USING PKARC AND PKXARC

PKARC   FAST!   Archive Create/Update Utility   Version 1.2   10-23-86
Copyright (c) 1986 PKWARE, Inc. All Rights Reserved. PKARC/h for help

    Usage: PKARC options archive [filename...]
    Options are:
     a = add files to archive   d = delete files from archive
     f = freshen files in archive   m = move files to archive
     u = update files in archive   v = display verbose listing of archive
     l = display software license   c = add/update file comments
     x = add/update archive comment

The A,F,M, and U options can be followed by a C and/or X to cause
prompting for the file comments and/or the archive comment. The V
option can be followed by a C for a verbose listing with file comments.

PKXARC   FAST!   Archive Extract Utility   Version 3.3   10-23-86
Copyright (c) 1986   PKWARE, Inc. All Rights Reserved. PKXARC/h for help

Extracts files from an archive to their original name, size, time, & date.

Usage: PKXARC [options] archive [d:path\] [-file...]
Options are:
/r = replace existing files   /v = verbose listing of archive(s)
/c = extract file(s) to the console /p = extract file(s) to the printer
/t = test archive integrity   /l = display software license

archive Archive file name, wildcards *,? ok. Default extension is .ARC
d:path\ Output drive and/or path.
-file   Name(s) of files to extract. Wildcards *,? ok.
Default is ALL files.

APPENDIX C

PROFILES OF WIND SPEED, LIQUID WATER CONTENT, TEMPERATURE, AND DRY - WET BULB TEMPERATURE

The following profiles are of several of the data channels recorded at SNI from 15 July through 25 July. Included are time, wind speed, liquid water content, dry bulb temperature, and wet bulb - dry bulb temperature. The vertical axis of each plot is altitude given in meters. The altitude is that of the balloon and not the instrument package.

Flight 1515

1400

Ascent of Flight 1515

0

5

Dry Bulb Temperature (C)

25

1400

Descent of Flight 1515

0

5

Dry Bulb Temperature (C)

25

41

Ascent of Flight 1515

Dry-Wet Temperature (C)

Descent of Flight 1515

Dry-Wet Temperature (C)

42

Ascent of Flight 1515

1400

0

0   Liquid Water Content (g/m^3)   .5

Descent of Flight 1515

1400

0

0   Liquid Water Content (g/m^3)   .5

43

Ascent of Flight 1515

Wind Speed (m/s)

Descent of Flight 1515

Wind Speed (m/s)

44

Flight 1609

1400

0

32300.6   time   41630.3

45

Ascent of Flight 1609

Dry-Wet Temperature (C)

Descent of Flight 1609

Dry-Wet Temperature (C)

Ascent of Flight 1609

Liquid Water Content (g/m^3)

Descent of Flight 1609

Liquid Water Content (g/m^3)

47

Flight 1617

1400

0

63732.8   time   69720.8

48

Ascent of Flight 1617

Dry Bulb Temperature (C)

Descent of Flight 1617

Dry Bulb Temperature (C)

49

Ascent of Flight 1617

1400

0

0   10
Dry-Wet Temperature (C)

Descent of Flight 1617

1400

0

0   10
Dry-Wet Temperature (C)

Ascent of Flight 1617

Liquid Water Content (g/m^3)

Descent of Flight 1617

Liquid Water Content (g/m^3)

Ascent of Flight 1617

Wind Speed (m/s)

Descent of Flight 1617

Wind Speed (m/s)

1400

Flight 1710

0

39620   Time   50426

1400

Ascent of Flight 1710

0

5   25

Dry Bulb Temperature (C)

1400

Descent of Flight 1710

0

5   25

Dry Bulb Temperature (C)

54

Ascent of Flight 1710

Dry-Wet Temperature (C)

Descent of Flight 1710

Dry-Wet Temperature (C)

55

Ascent of Flight 1710

1400

0

0   .5

Liquid Water Content (g/m^3)

Descent of Flight 1710

1400

0

0   .5

Liquid Water Content (g/m^3)

56

Ascent of Flight 1710

Wind Speed (m/s)

Descent of Flight 1710

Wind Speed (m/s)

57

Flight 1807

1400

0

28535.8   time   39462.8

Ascent of Flight 1807

1400

0

5   25

Dry Bulb Temperature (C)

Descent of Flight 1807

1400

0

5   25

Dry Bulb Temperature (C)

59

Ascent of Flight 1807

Dry-Wet Temperature (C)

Descent of Flight 1807

Dry-Wet Temperature (C)

60

Ascent of Flight 1807

1400

0

0   .5
Liquid Water Content (g/m^3)

Descent of Flight 1807

1400

0

0   .5
Liquid Water Content (g/m^3)

Ascent of Flight 1807

Wind Speed (m/s)

Descent of Flight 1807

Wind Speed (m/s)

62

Flight 1814

Time

1400

0

51363

56966

63

Ascent of Flight 1814

Dry Bulb Temperature (C)

Descent of Flight 1814

Dry Bulb Temperature (C)

Ascent of Flight 1814

Dry-Wet Temperature (C)

Descent of Flight 1814

Dry-Wet Temperature (C)

65

Ascent of Flight 1814

1400

0

0   .5

Liquid Water Content (g/m^3)

Descent of Flight 1814

1400

0

0   .5

Liquid Water Content (g/m^3)

Ascent of Flight 1814

Wind Speed (m/s)

Descent of Flight 1814

Wind Speed (m/s)

Flight 195

1400

0

20534.6   time   25262.6

68

1400 ─

Ascent of Flight 195

0 ─

5   Dry Bulb Temperature (C)   25

1400 ─

Descent of Flight 195

0 ─

5   Dry Bulb Temperature (C)   25

69

Ascent of Flight 195

1400

0

0   Dry-Wet Temperature (C)   10

Descent of Flight 195

1400

0

0   Dry-Wet Temperature (C)   10

70

Ascent of Flight 195

1400

0

0   .5

Liquid Water Content (g/m^3)

Descent of Flight 195

1400

0

0   .5

Liquid Water Content (g/m^3)

71

Ascent of Flight 195

1400

0

0   Wind Speed (m/s)   25

Descent of Flight 195

1400

0

0   Wind Speed (m/s)   25

72

Flight 1913

49282.6   time   57478.6

Ascent of Flight 1913

Dry Bulb Temperature (C)

Descent of Flight 1913

Dry Bulb Temperature (C)

74

Ascent of Flight 1913

Dry-Wet Temperature (C)

Descent of Flight 1913

Dry-Wet Temperature (C)

75

Ascent of Flight 1913

1400

0

0   .5

Liquid Water Content (g/m^3)

Descent of Flight 1913

1400

0

0   .5

Liquid Water Content (g/m^3)

76

Ascent of Flight 1913

1400

0

0   Wind Speed (m/s)   25

Descent of Flight 1913

1400

0

0   Wind Speed (m/s)   25

77

Flight 2008

1400

0

29519   time   36981

Ascent of Flight 2008

Dry Bulb Temperature (C)

Descent of Flight 2008

Dry Bulb Temperature (C)

79

1400

0

0   10
Dry-Wet Temperature (C)

Ascent of Flight 2008

1400

0

0   10
Dry-Wet Temperature (C)

Descent of Flight 2008

80

Ascent of Flight 2008

Liquid Water Content (g/m^3)

Descent of Flight 2008

Liquid Water Content (g/m^3)

81

Ascent of Flight 2008

Wind Speed (m/s)

Descent of Flight 2008

Wind Speed (m/s)

82

Flight 2017

64608   time   71074

Ascent of Flight 2017

1400

0

5   25

Dry Bulb Temperature (C)

Descent of Flight 2017

1400

0

5   25

Dry Bulb Temperature (C)

84

Ascent of Flight 2017

Dry-Wet Temperature (C)

Descent of Flight 2017

Dry-Wet Temperature (C)

Ascent of Flight 2017

1400

0

0   Liquid Water Content (g/m^3)   .5

Descent of Flight 2017

1400

0

0   Liquid Water Content (g/m^3)   .5

86

Ascent of Flight 2017

Wind Speed (m/s)

Descent of Flight 2017

Wind Speed (m/s)

87

Flight 2112

1400

0

46461.8   time   56144.8

Ascent of Flight 2112

1400

0

5

Dry Bulb Temperature (C)

25

Descent of Flight 2112

1400

0

5

Dry Bulb Temperature (C)

25

Ascent of Flight 2112

1400

0

0   Dry-Wet Temperature (C)   10

Descent of Flight 2112

1400

0

0   Dry-Wet Temperature (C)   10

Ascent of Flight 2112

Liquid Water Content (g/m^3)

Descent of Flight 2112

Liquid Water Content (g/m^3)

Ascent of Flight 2112

Wind Speed (m/s)

Descent of Flight 2112

Wind Speed (m/s)

92

Flight 2217

1400

0

63276.8   time   72462.8

93

1400

Ascent of Flight 2217

0

5   Dry Bulb Temperature (C)   25

1400

Descent of Flight 2217

0

5   Dry Bulb Temperature (C)   25

Ascent of Flight 2217

1400

0

0   Dry-Wet Temperature (C)   10

Descent of Flight 2217

1400

0

0   Dry-Wet Temperature (C)   10

95

Ascent of Flight 2217

Liquid Water Content (g/m^3)

Descent of Flight 2217

Liquid Water Content (g/m^3)

96

Ascent of Flight 2217

Wind Speed (m/s)

Descent of Flight 2217

Wind Speed (m/s)

97

Flight 239

1400

0

35000   time   44612

Ascent of Flight 239

Dry Bulb Temperature (C)

Descent of Flight 239

Dry Bulb Temperature (C)

99

Ascent of Flight 239

Dry-Wet Temperature (C)

Descent of Flight 239

Dry-Wet Temperature (C)

Ascent of Flight 239

Liquid Water Content (g/m^3)

Descent of Flight 239

Liquid Water Content (g/m^3)

101

Ascent of Flight 239

Wind Speed (m/s)

Descent of Flight 239

Wind Speed (m/s)

102

Flight 2315

1400

0

54275.8   time   60383.8

103

Ascent of Flight 2315

Dry Bulb Temperature (C)

Descent of Flight 2315

Dry Bulb Temperature (C)

104

Ascent of Flight 2315

Dry-Wet Temperature (C)

Descent of Flight 2315

Dry-Wet Temperature (C)

Ascent of Flight 2315

1400

0

0   .5

Liquid Water Content (g/m^3)

Descent of Flight 2315

1400

0

0   .5

Liquid Water Content (g/m^3)

Ascent of Flight 2315

Wind Speed (m/s)

Descent of Flight 2315

Wind Speed (m/s)

107

Flight 247

1400

0

27820.6   time   39452.2

108

Ascent of Flight 247

Dry Bulb Temperature (C)

Descent of Flight 247

Dry Bulb Temperature (C)

1400

0

Ascent of Flight 247

0   10
Dry-Wet Temperature (C)

1400

0

Descent of Flight 247

0   10
Dry-Wet Temperature (C)

110

Ascent of Flight 247

Liquid Water Content (g/m^3)

Descent of Flight 247

Liquid Water Content (g/m^3)

111

Ascent of Flight 247

Wind Speed (m/s)

Descent of Flight 247

Wind Speed (m/s)

112

Flight 2417

1400

0

62160.8   time   71024.8

1400

Ascent of Flight 2417

0

5   Dry Bulb Temperature (C)   25

1400

Descent of Flight 2417

0

5   Dry Bulb Temperature (C)   25

114

Ascent of Flight 2417

Dry-Wet Temperature (C)

Descent of Flight 2417

Dry-Wet Temperature (C)

Ascent of Flight 2417

Liquid Water Content (g/m^3)

Descent of Flight 2417

Liquid Water Content (g/m^3)

Ascent of Flight 2417

1400

0

0   Wind Speed (m/s)   25

Descent of Flight 2417

1400

0

0   Wind Speed (m/s)   25

117

Flight 257

1400

0

28474.8   time   37458.8

Ascent of Flight 257

Dry Bulb Temperature (C)

Descent of Flight 257

Dry Bulb Temperature (C)

Ascent of Flight 257

Dry-Wet Temperature (C)

Descent of Flight 257

Dry-Wet Temperature (C)

1400

Ascent of Flight 257

0

0

Liquid Water Content (g/m^3)

.5

1400

Descent of Flight 257

0

0

Liquid Water Content (g/m^3)

.5

121

Ascent of Flight 257

Wind Speed (m/s)

Descent of Flight 257

Wind Speed (m/s)

122